

Supporting Information

Controlled Covalent Functionalization of Thermally Reduced Graphene Oxide To Generate Defined Bifunctional 2D Nanomaterials

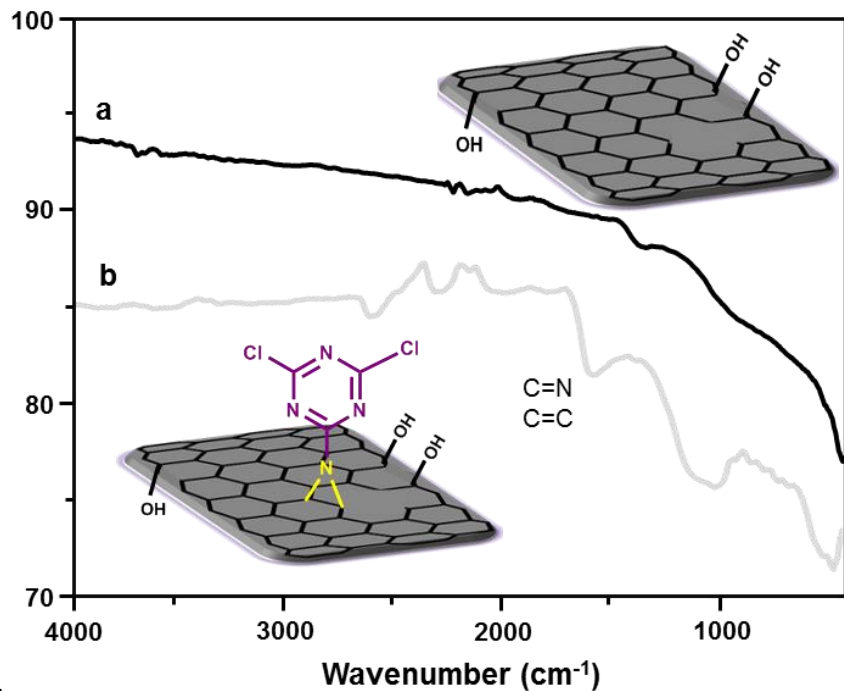
Abbas Faghani, Ievgen S. Donskyi, Mohammad Fardin Gholami, Benjamin Ziem, Andreas Lippitz, Wolfgang E. S. Unger, Christoph Böttcher, Jürgen P. Rabe, Rainer Haag, and Mohsen Adeli**

anie_201612422_sm_miscellaneous_information.pdf

Supporting Information

Table of Contents

TRGO-hPG_L (0.02 g) was dispersed in DMF (20 mL) by sonication for 30 minutes. Then, Et₃N (0.01 mL, 7.1
15

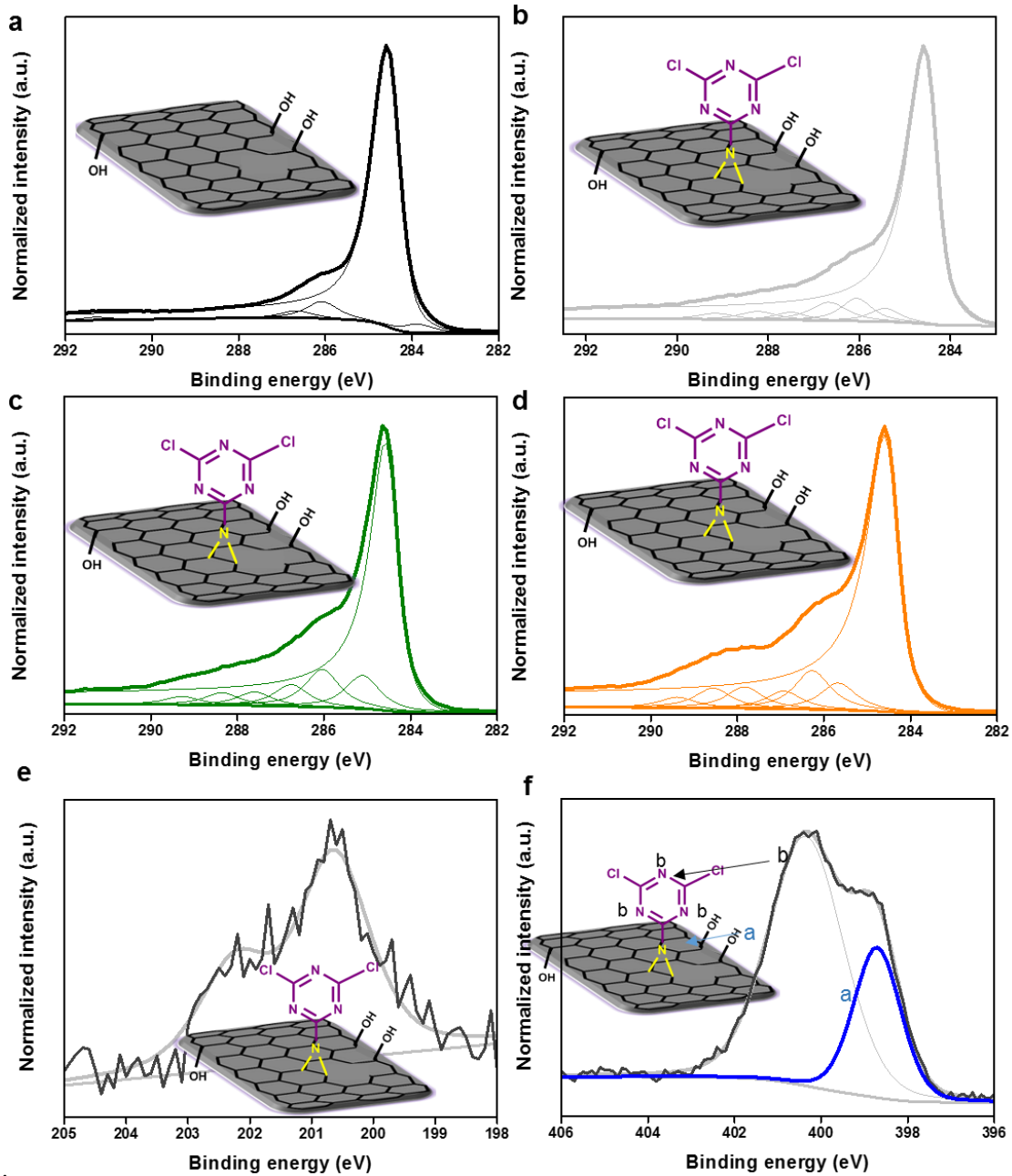


16

16 Figure S1.

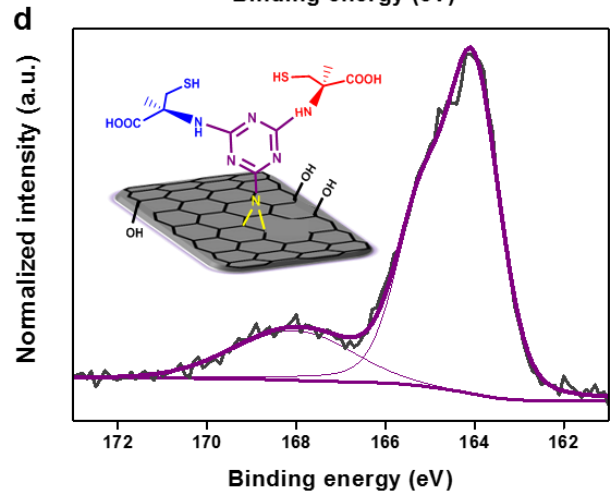
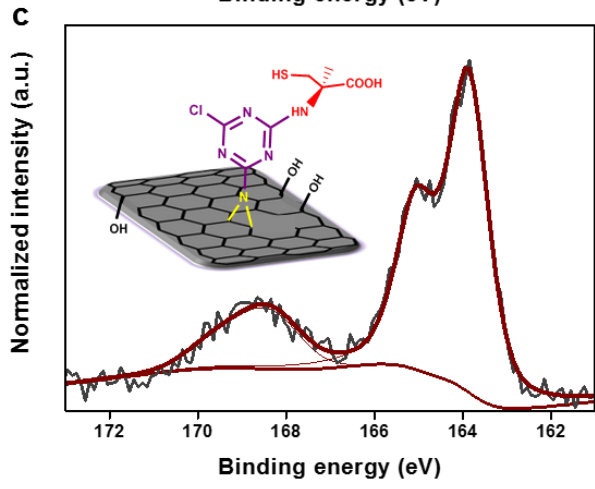
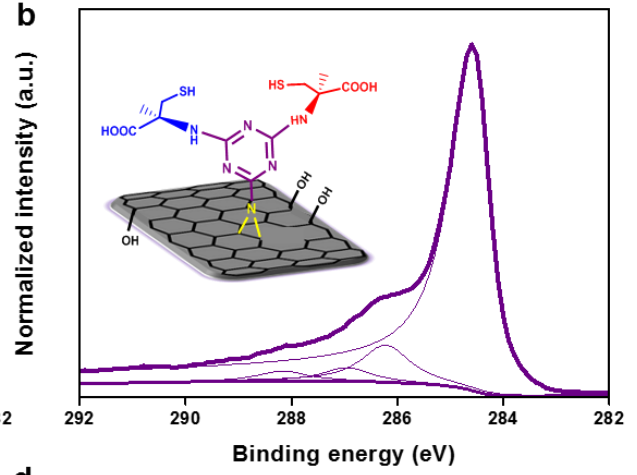
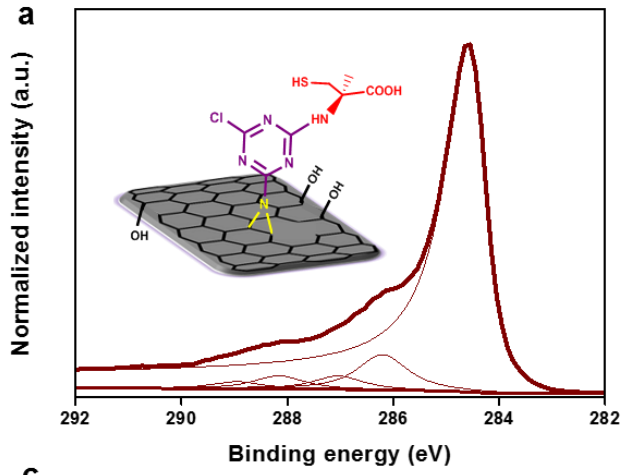
17 Table S1.

22 Table S4.

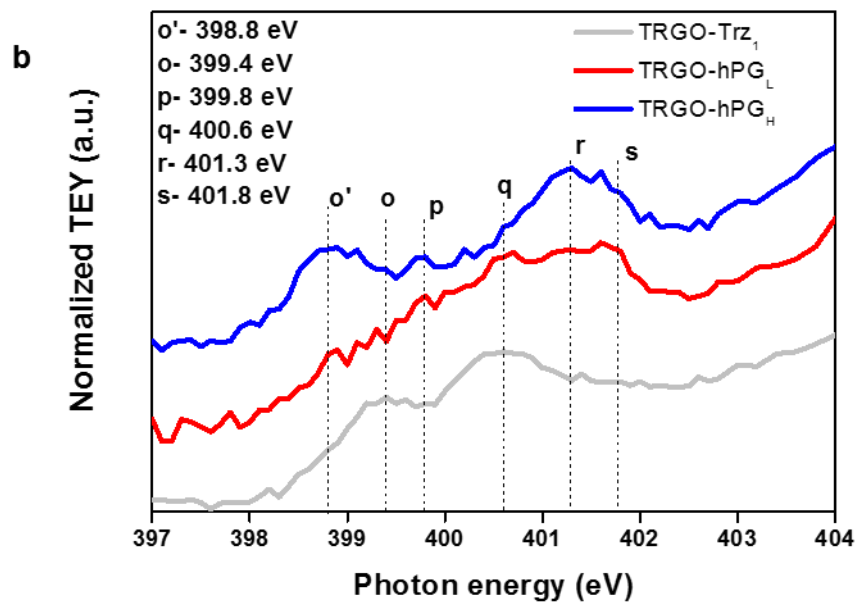
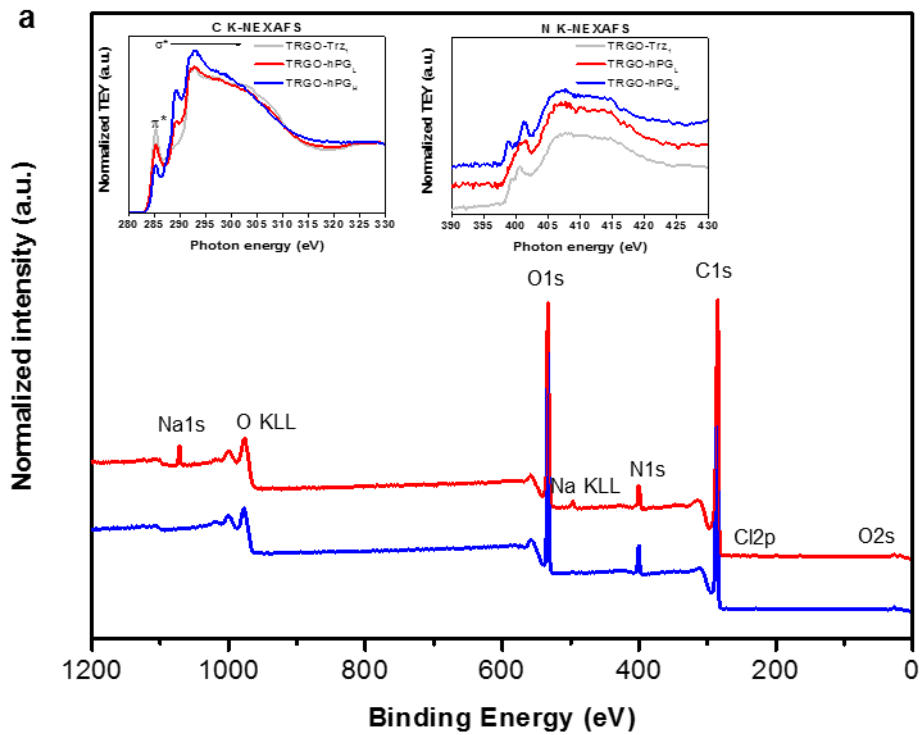


26

26 Figure S5.

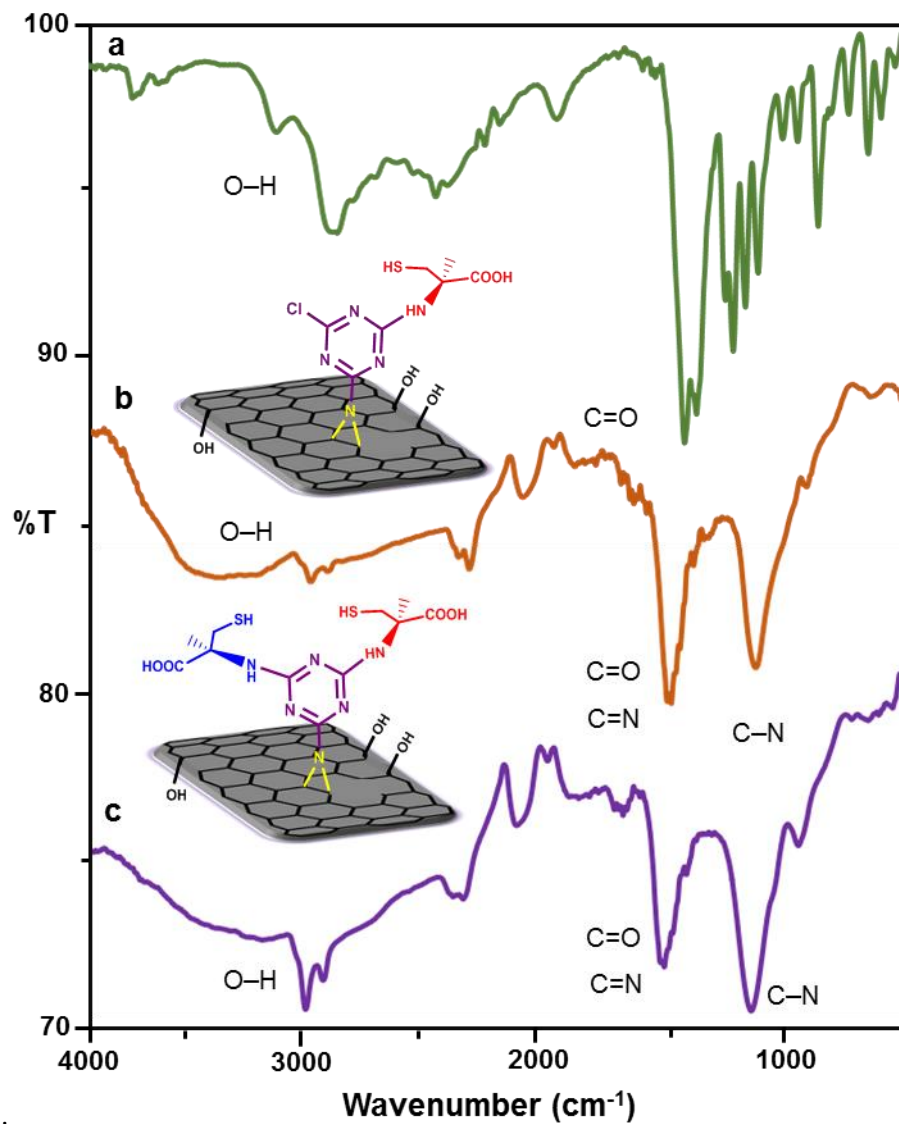


28.....



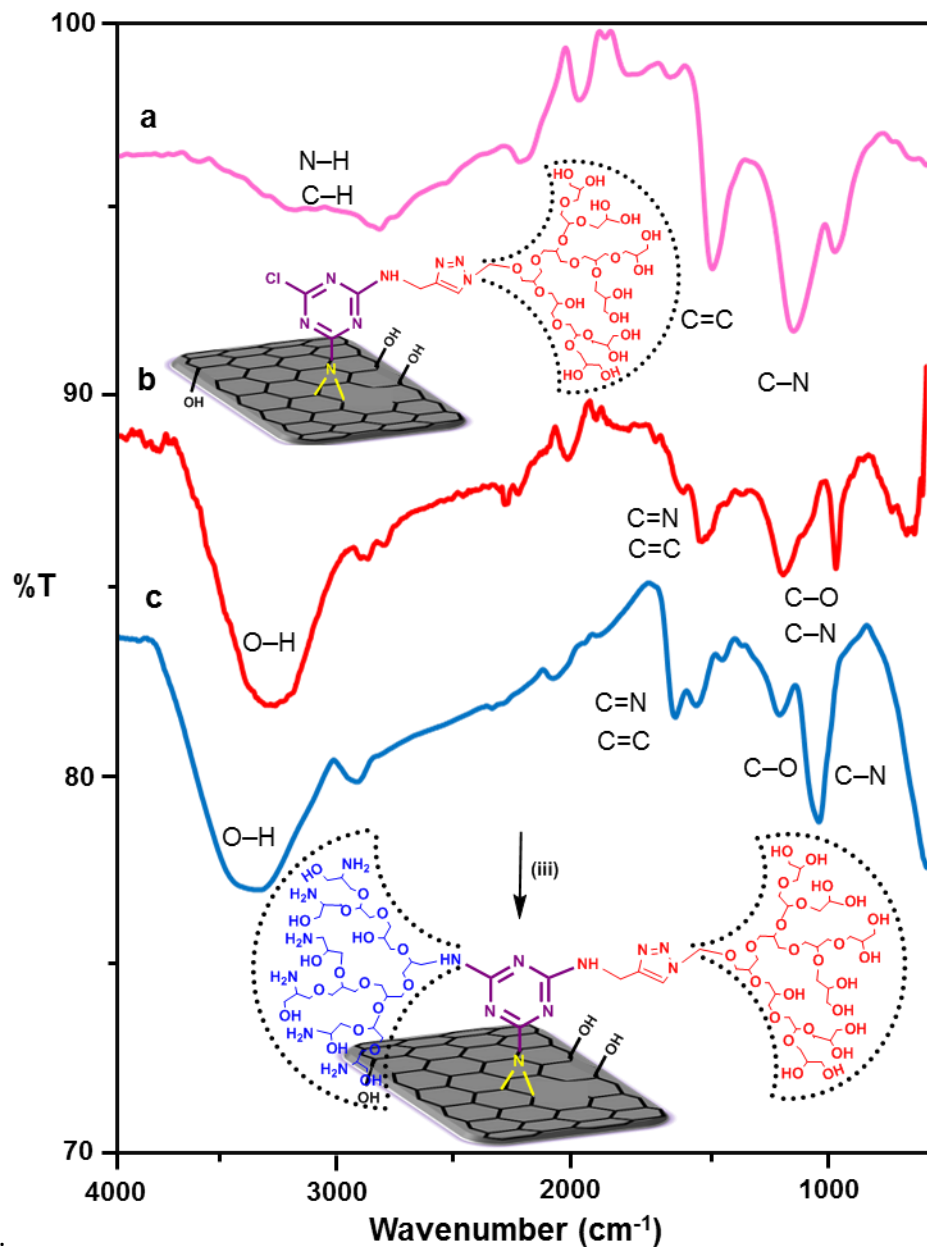
30

30 Figure S9.



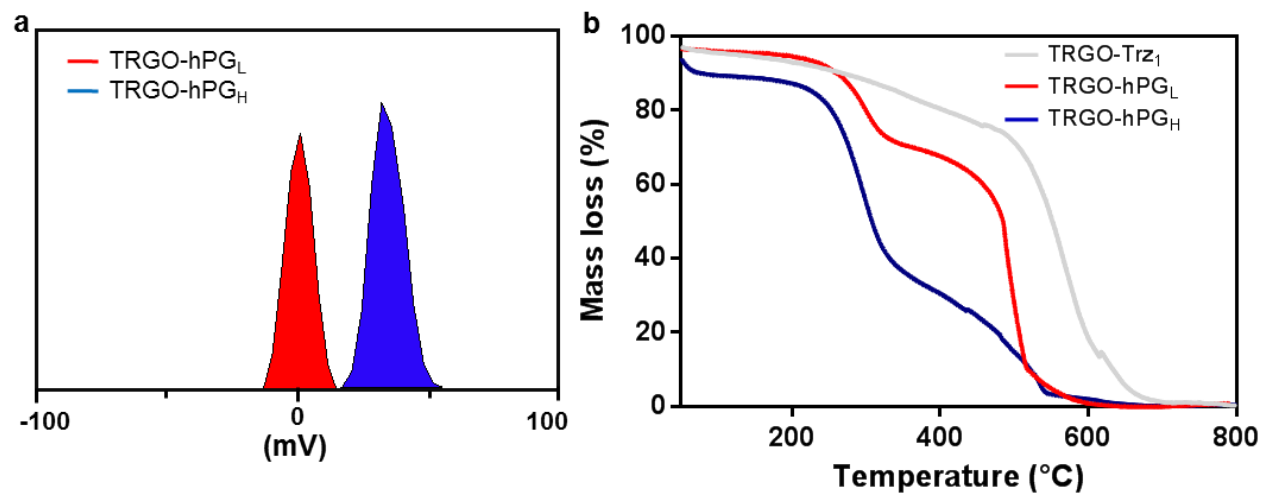
35

35 Figure S13.



38

38 Figure S14.



40
 40 Figure S15. a,
 41 Figure S16.
 43 Figure S17.

Experimental Section

Materials

Chemicals: 2,4,6-trichloro-1,3,5-triazine (cyanuric chloride or triazine), propargylamine, Copper(II) sulfate-pentahydrate ($\text{CuSO}_4 \cdot 5\text{H}_2\text{O}$), sodium hydroxide (NaOH), triethylamine (Et_3N), sodium ascorbate, β -cyclodextrin, ethylenediamine, *p*-Toluenesulfonyl chloride, rhodamine 6G, L- and D- cysteine, were purchased from Across Organics (Geel, Belgium). Dimethylformamide (DMF), methanol, chloroform, acetone, Phosphate-buffered saline (PBS) and N-methyl-2-pyrrolidone were purchased from Merck (Germany). Suspension of gold nanoparticles (5 nm diameter) was stabilized in citrate buffer, sodium azide, ethylenediaminetetraacetic acid (EDTA) and dialysis bags (benzoylated cellulose, MWCO 100 - kDa) were purchased from Sigma-Aldrich (Schnelldorf, Germany). Thermally reduced graphene oxide (TRGO) was prepared according to published procedure and provided by R. Mülhaupt et al.^[1] The elemental analysis shows that carbon and hydrogen contents of TRGO, used in the present work, are 87.75% and 1.74%, respectively (Table S1). According to reported data in literature carbon, hydrogen and oxygen contents of thermally reduced graphene oxide (750 °C) are 85%, 0.39% and 14.37%, respectively. Clearly, our recorded data and those reported in literature are close enough and difference is negligible. According to elemental analysis and within the experimental errors the ratio of oxygen/carbon atoms for TRGO is roughly 1/6. This oxygen content is mostly assigned to the hydroxyl functional groups at the edges or defect sites. Thermal decomposition at 750 °C results in the CO_2 formation and expansion of layers and finally an amorphous carbon framework. Additional oxygen content together with thermal treatment causes creation of five membered rings within an activated carbon network. Therefore, hole formation is expected and the perfect hexagonal structure of graphene is no longer present. In such 2D structure reaction at the edges and defect sides can be assumed.

Fourier transform infrared spectroscopy (FT-IR): IR spectra were recorded using a JASCO spectrometer. Ultrasonic bath (Model: SONOREX, RK255 HZ, Made in Germany) was used to disperse materials in solvents.

UV-Vis spectroscopy: The measurements were performed on a Shimadzu UV-2450 spectrophotometer at room temperature. A 1cm path length quartz cuvette was used in the experiments. In our experiment, the absorbance process was pursued in milli-Q water (pH 7.4) at 25 °C.

Circular dichroism spectroscopy (CD): Graphenic samples were analyzed in deionized water (pH = 7). CD spectra were measured on a J-810 spectropolarimeter (Jasco GmbH) equipped with a temperature controlled quartz cell of 0.1 cm path length. The spectra were recorded from three scans obtained within wavelengths from 190 to 240 nm. For measurement the concentrations were: 1 mg/mL in deionized water at 25 °C.

Thermal gravimetric analysis (TGA): TGA measurements were recorded by a STA 409 apparatus (Linseis) at temperatures range 25-800 °C with a 5 °C/min heating rate under argon gas.

Zeta potential measurement: TRGO derivatives were sonicated for 15 min before zeta potential measurements and all measurements were performed using Malvern Zetasizer Nano machine (Brookhaven Instruments Crop) spectrometer operating under 633 nm laser irradiation at 25 °C. The zeta potential measurements were carried out at pH 7.

Elemental analysis: Elemental analysis was performed using ELEMENTAR apparatus with three columns and detector for carbon, nitrogen, hydrogen and sulfur elements.

Scanning force microscopy (SFM): Dispersions of TRGO-Trz₁-hPG_L and TRGO-Trz₁-hPG_H in water were prepared using ultrasonication. TRGO and TRGO-Trz₁, used as references, were ultrasonicated in a chloroform solution (1 mg/mL). Dispersions were spin-casted onto a freshly cleaved mica surface (Ratan mica Exports, V1 (optical quality)) or highly oriented pyrolytic graphite surface (HOPG, grade ZYA, Advanced Ceramics). For this, a droplet of solution was applied onto a freshly cleaved mica surface for a few seconds and then spun off. The scanning force microscope (Bruker Corporation, Multimode, Nanoscope 8) was operated with an E-scanner (unless specified differently) in tapping mode (TM) and quantitative nanomechanical mapping mode (QNM) at typical rates of 5-15 minute per image. Relative humidity (RH) and temperature of the SFM lab were measured using (testo 635 of Testo GmbH, Error of ±2.5%) close to the Multimode head. Silicon cantilevers were used with typical resonance frequencies of 70 kHz and spring constants of 2 N/m. The tips exhibited a typical apex radius of 7 nm with an

upper limit of 10 nm, as specified by the manufacturer (Olympus Corporation). For the QNM, the sensitivity of the cantilevers was calibrated over a sapphire surface (supplied by Bruker Corporation) and later thermally tuned. Typical spring constants of the cantilevers were within 1.7-2.1 N/m. The SFM images were processed and analyzed with SPIP (Image Metrology A/S) image processing software. RH and temperatures during the SFM imaging were within 35-40% and 23.5-25 °C, respectively.

Cryogenic transmission electron microscopy (Cryo-TEM): Cryo-TEM images were done using perforated (1 μm hole diameter) carbon film-covered microscopical 200 mesh grids (R1/4 batch of Quantifoil, Micro Tools GmbH, Jena, Germany) that were hydrophilised by 60 s glow discharging at 8 W in a BALTEC MED 020 device. Then 5 μl of the corresponding samples were pipetted to the hydrophilised grid, and the supernatant fluid was immediately removed with a piece of filter paper until an ultrathin layer of the sample solution was obtained spanning the holes of the carbon film. The sample was instantly vitrified by plunging the grids into liquid ethane using a guillotine-like apparatus. The vitrified sample was subsequently transferred under liquid nitrogen into a Tecnai F20 TEM (FEI Company, Oregon) equipped with a field emission gun and is operating at 160 kV by the use of a Gatan tomography Cryo-holder (Model 914). Microscopy was carried out at a 94 K sample temperature using the low-dose protocol of the microscope. Micrographs were taken with an FEI Eagle 4k \times 4k CCD camera using a twofold binning mode. To generate stereo images the same image section was recorded at two different tilt angles (4° and -4°) using the compustage of the microscope. The resulting micrographs were aligned using the software StereoPhoto Maker (Masuji Suto, Japan).

X-ray photoelectron spectroscopy (XPS): XP spectra were recorded on a Kratos Axis Ultra DLD spectrometer using a monochromated Al $K\alpha$ X-ray source at an analyzer pass energy of 80 eV for survey spectra and 20 eV for high-resolution core-level spectra which were recorded in FAT (fixed analyser transmission) mode. The electron emission angle was 60° and the source-to-analyzer angle was 60° . The binding energy scale of the instrument was calibrated following a Kratos Analytical procedure which uses ISO 15472 binding energy data. Spectra were recorded by setting the instrument to the hybrid lens mode and the slot mode providing approximately a 300 \times 700 μm^2 analysis area. Charge neutralization had been used. All XPS spectra were processed with the UNIFIT program (version 2017). A Gaussian/Lorentzian sum function peak shape model GL (30) was used in combination with a Shirley background. If not otherwise

denoted the L-G mixing for component peaks in all spectra were constrained to be identical. The S2p core level spectra were fitted with doublets of fixed separation of 1.2 eV, an area ratio of S2p3/2: S2p1/2 = 2:1^[2] and equal FWHMs for S2p3/2 and S2p1/2. The FWHM of the high energy Cl2p and S2p doublets were allowed to vary in a window of 1–1.6 times the FWHM of the low energy doublet. Peak fitting of C1s spectra was performed by using an asymmetric peak shape model for the graphene C1s component. After peak fitting of the C1s spectra, all the spectra were calibrated in reference to the graphene C1s component at a binding energy of 284.6 eV (static charge reference). Gold substrates for the XPS analysis were cleaned in a piranha solution (1:4) 30% H₂O₂: 98% H₂SO₄ (v/v) during ultrasonication at room temperature for 10 minutes. Then they were washed with the DI water 5 times and with acetone 2 times. After drying 12 hours the studied compounds were dissolved in methanol and dropwise evenly distributed over the surface of gold substrates.

NEXAFS: NEXAFS measurements have been carried out at the synchrotron radiation source BESSY II (Berlin, Germany). NEXAFS spectra were acquired at the HE-SGM monochromator dipole magnet CRG beamline. NEXAFS spectra were acquired in total energy electron yield (TEY) mode using a channel plate detector.^[3] The resolution $E/\Delta E$ of the monochromator at the carbonyl π^* resonance ($h\nu = 287.4$ eV) was in the order of 2500. Both C K- and N K-edges were measured at 55° incident angle of the linearly polarized synchrotron light beam. Raw spectra were divided by ring current and monochromator transmission, the latter obtained with a freshly sputtered Au sample.^[3] Alignment of the energy scale was achieved by using an I₀ feature referenced to a C1s $\rightarrow \pi^*$ resonance at 285.4 eV measured with a fresh surface of HOPG (highly ordered pyrolytic graphite, Advanced Ceramic Corp, Cleveland, USA).^[4] If not otherwise denoted all NEXAFS spectra are shown after subtraction of the pre-edge signal followed by normalization of the post-edge count rates to one.^[3]

Synthesis and Characterization

Synthesis of hyperbranched polyglycerolamine (hPG-NH₂)_{50%}

Amino-functionalized hyperbranched polyglycerol (hPG-NH₂)_{50%} was synthesized according to reported procedure in literature. In a three-step protocol, hyperbranched polyglycerol (PG, molecular weight of $M_n = 7,200$ g.mol⁻¹, PDI < 1.2, and a degree of branching of ~50%) was

mesylated and subsequently transformed to azido-functionalized derivative through reaction with sodium azide in aqueous solution. Finally reduction of azide functional groups to amino analogs using triphenylphosphine resulted in TRGO-hPG-NH₂.^[5,6] Yield 70%.

Functionalization of TRGO by triazine (TRGO-Trz)

2,4,6-trichloro-1,3,5-triazine 10 g (0.054 mol) was dissolved in 30 mL N-methyl-2-pyrrolidone (NMP) and then sodium azide 3.52 g (0.054 mol) (dispersed in 10 mL of the same solvent) was added at 0 °C and mixture stirred for 20 minutes. TRGO, 0.4 g was added to the mixture and stirred at 0 °C for 2 hours. The temperature was raised to 60 °C and the mixture was stirred for additional 10 hours. The product was then washed with acetone (4 × 10 mL) and water (4 × 10 mL) using centrifugation at 8,000 rpm for 10 minutes, then dried by lyophilization. Yield 73%.

Increasing the density of triazine functional groups on TRGO

TRGO-Trz 0.1 g was added to NMP (50 mL) and sonicated at 25 °C for 1 hour. Then a solution of azido-triazine prepared as described above was added dropwise at 0 °C to this dispersion. The mixture was stirred at 0 °C, 25 °C and 60 °C each for 1, 2 and 14 hours, respectively. The mixture was centrifuged and washed with water, acetone and chloroform until a clear supernatant was obtained. Yield 68%.

Control experiments for the calculation of DF of TRGO-Trz

TRGO 0.2 g was added to NMP (20 mL) and stirred at 0 °C for 2 hours. Then temperature was raised to 60 °C and the mixture was stirred for additional 10 hours. The product was then washed with acetone (4 × 10 mL) and water (4 × 10 mL) using centrifugation at 8,000 rpm for 10 minutes. Then it was dried by lyophilization. The nitrogen contents for control experiments are added to the table 1.

Synthesis of TRGO-propargyl

TRGO-Trz₁ 0.4 g was added to DMF (150 mL) and sonicated for 40 minutes. Then propargylamine (2.15 g, 2.50 mL, 0.039 mol) and triethylamine (Et₃N) (5.4 g, 7.5 mL, 0.05 mol) were added stepwise at room temperature. The mixture was stirred for 2 hours and sonicated for 30 minutes at room temperature and then stirred at 25 °C for 24 hours. The mixture was centrifuged at 11,000 rpm for 20 minutes and the precipitate was washed with water, acetone,

chloroform, and methanol (each 4×10 mL). The product was dried by lyophilization. Yield 93%.

Synthesis of TRGO-hPGL

TRGO-Trz₁-propargyl 0.3 g was added to DMF (70 mL) and sonicated for 1 hour at room temperature. Hyperbranched polyglycerol with azide functional groups (hPG-N₃, M_n = 7,200 g.mol⁻¹ and 4% azide groups) (2 g, 3.11×10^{-4} mol) was added to this mixture and stirred for 30 minutes. After addition of sodium ascorbate (1.4×10^{-4} mol, 0.027 g) and CuSO₄.5H₂O (1.4×10^{-4} mol, 0.024 g), the mixture was sonicated for additional 20 minutes and stirred at room temperature for 1 hour and then at 50 °C for 24 hours. The reaction product was centrifuged at 11,000 rpm for 1 hour. The precipitate was washed by water, acetone, chloroform, and methanol (each 5×15 mL) and then centrifuged at 11,000 rpm for 2 hours. Then product was mixed with ethylenediaminetetraacetic acid in water and stirred for 12 hours. The product was dialyzed with a molecular weight cut-off (MWCO 100 kDa) bag against water for 3 days. The solvent was evaporated and the product was dried by lyophilization. Yield 80%.

Synthesis of TRGO-hPGH

TRGO-hPGL 0.08 g was dispersed in NMP (25 mL) and sonicated at room temperature for 2 hours. The hPG-(NH₂)_{50%} (M_n = 7,200 g.mol⁻¹) (0.02 g) was dissolved in NMP (15 mL) and added to the TRGO-hPGL dispersion at 25 °C. The mixture was stirred at this temperature for 2 hours and then Et₃N (0.5 mL, 0.003 mol) was added to the reaction flask and stirred at 60 °C for 48 hours. The product was precipitated in acetone and dialyzed (MWCO 100 kDa) against water for 3 days. Purification was done by washing with water, methanol and acetone (each 5×15 mL) and then collected from centrifugation at 11,000 rpm for 1 hour. The solvent was evaporated and product was dried by lyophilization. Yield 81%.

Gold nanoparticles (GNPs) incubation

TRGO-hPGH 0.05 g was dispersed in Water (20 mL) and sonicated for 30 minutes. Gold nanoparticles with citrate shell in PBS (3 mL) were added to the TRGO-hPGH dispersion in water at 25 °C. The mixture was stirred at this temperature for 2 hours and then collected from centrifugation at 6,000 rpm for 20 minutes. Furthermore, neutrally charged TRGO-hPGL was incubated with GNPs in a similar manner to incubation of TRGO-hPGH as control.

Synthesis of TRGO-L-Cys

TRGO-Trz₁ 0.1 g was dispersed in DMF (50 mL) and sonicated for 45 minutes at room temperature. Then L-cysteine (1 g, 8.2×10^{-3} mol) and Et₃N (1.72 mL, 12.3×10^{-3} mol) were added to the mixture and stirred at 25 °C for 2 days. The product was precipitated by centrifugation at 11,000 rpm for 15 minutes and dialyzed (MWCO 100 kDa) for 7 days against the diluted alkali water (0.1 M, NaOH). The product was lyophilized for 24 hours. Yield 89% after dialysis. Furthermore, TRGO-L, D-Cys was synthesized in a similar manner to synthesis of TRGO-L-Cys. D-cysteine (1 g, 8.2×10^{-3} mol) and Et₃N (1.72 mL, 12.3×10^{-3} mol) were added to the mixture and stirred at 60 °C for 2 days. Yield 85% after dialysis.

A control for the stepwise post-modification of TRGO-Trz

TRGO-L-Cys 0.1 g was dispersed in DMF (50 mL). Then D-cysteine (1 g, 8.2×10^{-3} mol) and triethylamine (1.72 mL, 12.3×10^{-3} mol) were added to the dispersion and the mixture was stirred at 25 °C for 2 days. The purification of the product was the same as for TRGO-L-Cys.

Synthesis of TRGO-D-Cys

TRGO-Trz₁ 0.1 g was dispersed in DMF (50 mL) and sonicated for 45 minutes at room temperature. Then D-cysteine (1 g, 8.2×10^{-3} mol) and triethylamine (1.72 mL, 12.3×10^{-3} mol) were added to the mixture and stirred at 25 °C for 2 days. The product was precipitated by centrifugation at 11,000 rpm for 15 minutes and dialyzed for 7 days against the diluted alkali water (0.1 M, NaOH). The product was lyophilized for 24 hours. Yield 86% after dialysis.

Synthesis of TRGO-Trz with 0.5% nitrogen content (TRGO-Trz_L)

TRGO 0.065 g was dispersed in NMP (12 mL) and sonicated for 30 minutes. Then 2,4,6-trichloro-1,3,5-triazine 0.52 g (2.8×10^{-3} mol) was dissolved in NMP (15 mL) and then sodium azide (0.18 g, 2.8×10^{-3} mol) was added to this solution at 0 °C. These solutions were mixed at 0 °C. Afterwards, mixture was stirred at 60 °C for 10 minutes to obtain TRGO-Trz_L. Purification of the product was the same as for other TRGO-Trz samples.

Post-modification of TRGO-Trz_L by hPG-NH₂ 10%

TRGO-Trz_L with low and high polyglycerol coverage were synthesized according to procedures explained for the preparation of TRGO-hPG_L and TRGO-hPG_H, respectively.

Synthesis of the amino-β-cyclodextrin (β-CD-NH₂):

Mono-6-deoxy-6-(p-tolylsulfonyl)- β -cyclodextrin (6-OTs-CD) was prepared according to the reported procedures in literature.^[7,8] Briefly, β -CD (1 g, 8.8×10^{-3} mol) was suspended in 40 mL water at room temperature. Then 5 mL of NaOH aqueous solution (1.2×10^{-1} M) was added dropwise to the suspension upon stirring. Then, p-TSCl (0.15 g, 6.8×10^{-5} mol) dissolved in acetonitrile (10 mL) was added to the mixture. The mixture was stirred for 4 hours at room temperature. Afterwards, the pH value of the mixture was adjusted at 7.0 using 10% HCl. The precipitate was filtered and recrystallized at 60 °C for three times two times to obtain 6-OTs- β -CD.

In order to obtain β -CD-NH₂, 6-OTs- β -CD (0.5 g) was heated in excess of anhydrous ethylenediamine (15 mL) at 70 °C for 5 hours under inert atmosphere. Then reaction was cooled down to the room temperature and 25 mL of cold acetone was added to the mixture. The precipitate was collected by filtration and washed by cold acetone (3×10). The solid was dried under vacuum overnight to obtain β -CD-NH₂. Yield: 31 %

Conjugation of β -CD-NH₂ to TRGO-hPGL (TRGO-hPG-CD):

TRGO-hPGL (0.02 g) was dispersed in DMF (20 mL) by sonication for 30 minutes. Then, Et₃N (0.01 mL, 7.1×10^{-5} mol) was added into the dispersion and it was stirred for 20 min. β -CD-NH₂ (0.07 g, 5.8×10^{-5} mol) was added to the mixture and it was stirred for additional 12 hours at 60 °C. Finally, reaction was cooled down and mixture was washed with water (2×15) and dialyzed (MWCO: 10 KDa) against water for 3 days. Yield: 77 %

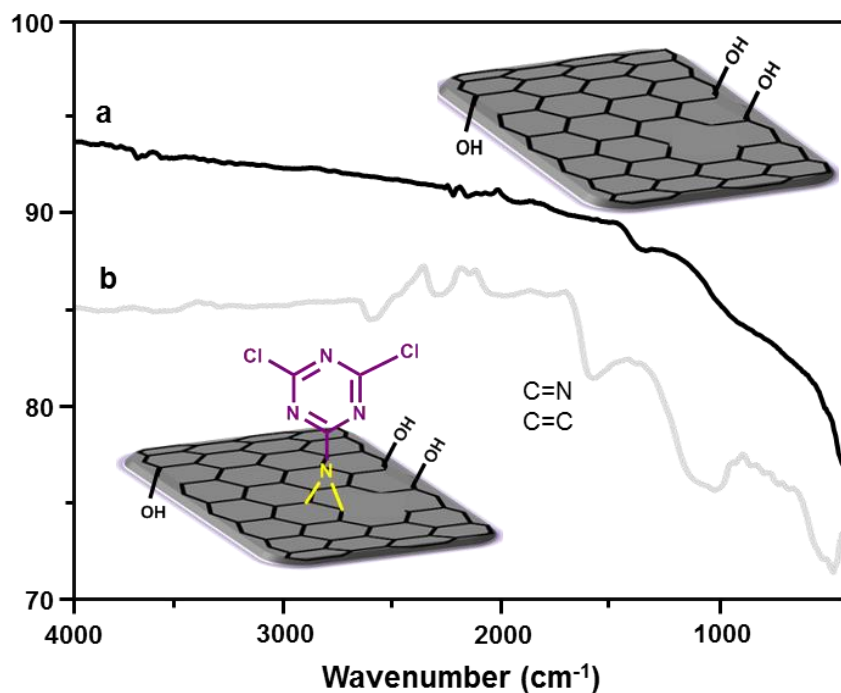


Figure S1. **a**, and **b**, IR spectra of reduced graphene oxide (TRGO) and TRGO-Trz₁, respectively. A broad absorbance band for C=C and C=N bonds of TRGO and triazine moieties is observed at 1,501-1,612 cm⁻¹, respectively. Absorbance bands at 740 and 1,075-1,209 cm⁻¹ are assigned to the C-Cl and C-N bonds of the triazine groups, respectively.

Calculations of degree of functionalization (DF):

$$DF = \frac{\text{number of triazine groups}}{\text{number of carbon atoms of graphene}}$$

1. Number of triazine groups: expressed as N wt.% in elemental analysis
2. Number of carbon atoms of TRGO: expressed as C wt.% in elemental analysis

Table S1. Nitrogen, carbon and hydrogen contents of the functionalized and non-functionalized TRGO obtained by elemental analysis.

Compound	N (wt.%)	C (wt.%)	H (wt.%)
TRGO	0.06	87.75	1.74
TRGO-Trz ₁	7.30 ^a	76.26	2.73
TRGO-Trz ₂	8.77 ^b	65.58	2.92
TRGO-Trz ₃	12.15 ^c	66.99	3.45

a, b and c: nitrogen contents of TRGO-Trz₁, TRGO-Trz₂ and TRGO-Trz₃ after subtraction the nitrogen content originated from trapped NMP.

Mass percent of nitrogen (N wt.%) is an indicator for DF of TRGO-Trz and strongly depends on the number of reaction runs.

In order to subtract the nitrogen content of NMP trapped in the products, control experiments were performed by incubation of TRGO derivatives with NMP in the same conditions as functionalization reaction was occurred.

Table S2. Nitrogen content measured by elemental analysis and DF of TRGO-Trz obtained at different runs of nitrene [2+1] cycloaddition reaction.

Compound	Run of reaction	N (wt.%)	DF ^a	DF ^b	DF ^c
TRGO	0	0.06	0	0	-
TRGO-Trz ₁	1	7.30	1:50	1:48	-
TRGO-Trz ₂	2	8.77	1:39	1:39	-
TRGO-Trz ₃	3	12.15	1:25	1:28	-
TRGO-Trz _L	-	0.50	-	-	1:920

^aDF based on nitrogen content obtained by elemental analysis, ^bDF based on mass loss in TGA thermograms, ^cDF based on nitrogen content obtained by XPS analysis.

DF of TRGO-Trz₁, TRGO-Trz₂ and TRGO-Trz₃ was calculated based on (N wt.%) content as following:

For TRGO-Trz₁:

X 56 (Mass of N atoms of one triazine group)

100 7.3

X = 767.12 (Mass of a building block of TRGO-Trz₁)

767.12 – 163.5 = 603.62

DF = 554.44/12 = 50.3

163.5 is the mass of the triazine group on the TRGO surface



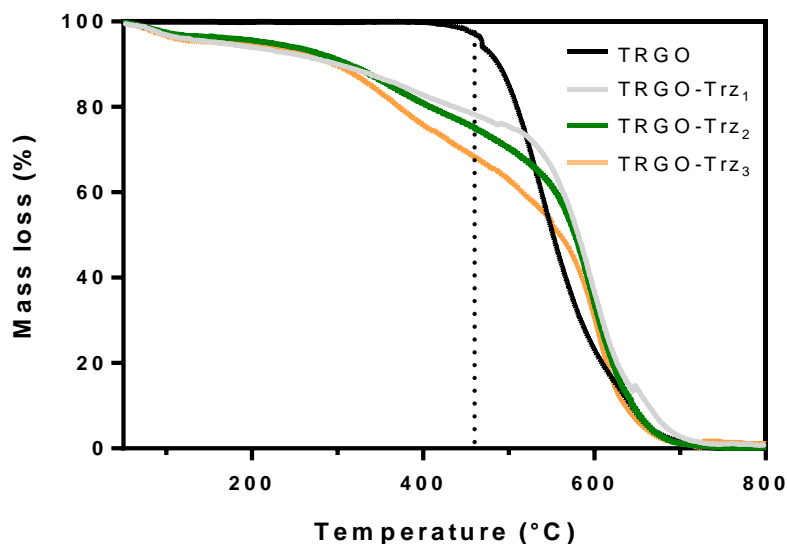


Figure S2. TGA thermograms of TRGO, TRGO-Trz₁, TRGO-Trz₂, and TRGO-Trz₃.

Calculation of DF based on TGA thermograms:

TGA revealed an increase in the mass loss versus the number of nitrene [2+1] cycloaddition reaction runs. This confirms the increase in the DF of the TRGO-Trz after each step. Mass losses of the TRGO-Trz₁, TRGO-Trz₂ and TRGO-Trz₃ at 450 °C, temperature at which TRGO starts to decompose, are ~22 wt.%, ~26 wt.% and ~33 wt.%, respectively. DF of TRGO-Trz could be calculated based on those mass losses as following:

For TRGO-Trz₁ (grey thermogram):

X 163.5 (Mass of the one triazine group on the TRGO surface)

100 22 (Mass loss of the TRGO-Trz₁)

X = 743.18 (Mass of a building block of TRGO-Trz₁)

743.18 – 163.5 = 579.68

DF = 579.68/12 = 48.3



Table S3. Interpretation of the fitted components in the highly resolved XPS spectra shows a wide number of possible component peaks assigned to different carbon species.

Sample	Spectrum	Binding energy	L-G Mixing	FWHM	Interpretation	Relat. Area	Abs. Area [cps*eV]
TRGO	C1s	284.6	0.67	0.77	C-C sp ²	0.89	38,852
		283.9	0.69	0.86	C-C sp ² diff. charged	0.03	1,122
		286.1	0.69	0.86	C-O-C, C-O-H	0.05	2,247
		286.7	0.69	0.86	C=O, O-C-O	0.02	923
		291.3	0.69	0.86	π - π^* shake up	0.01	382
TRGO-Trz ₁	C1s	284.6	0.78	0.79	C-C sp ²	0.81	35,699
		285.4	0.79	0.80	C-N=C	0.03	1,371
		286.1	0.79	0.80	C-O-C, C-O-H	0.05	2,361
		286.7	0.79	0.96	C-Cl	0.05	2,247
		287.5	0.79	0.80	C=O, O-C-O	0.02	795
		288.2	0.79	0.96	NH-C=O	0.02	1,007
		289.2	0.79	0.96	COO, COOH	0.02	727
	N1s	398.7	0.18	1.29	C-N-C	0.28	1,873
		400.4	0.18	2.03	C-N=C, N-C=O	0.72	4,873
	Cl2p	200.6	0.48	1.38	C-Cl	1	201
TRGO-Trz ₂	C1s	284.6	0.91	0.78	C-C sp ²	0.70	29,003
		285.1	0.84	0.94	C-N=C	0.08	3,234
		286.0	0.84	0.94	C-O-C, C-O-H	0.09	3,687
		286.8	0.84	0.94	C-Cl	0.05	2,127
		287.6	0.84	0.94	C=O, O-C-O	0.03	1,339
		288.4	0.84	0.94	NH-C=O	0.03	1,206
		289.3	0.84	0.94	COO, COOH	0.02	807
TRGO-Trz ₃	C1s	284.6	0.87	0.89	C-C sp ²	0.72	32,224
		285.7	0.87	0.98	C-N=C	0.06	2,504
		286.3	0.87	0.98	C-O-C, C-O-H	0.08	3,609
		286.9	0.87	0.98	C-Cl	0.04	1,650
		287.8	0.87	0.98	C=O, O-C-O	0.04	2,010
		288.6	0.87	0.98	NH-C=O	0.04	1,853
		289.4	0.87	0.98	COO, COOH	0.02	973
TRGO-Trz _L	C1s	284.6	0.77	0.82	C-C sp ²	0.8780.	29,589
		283.8	0.77	0.82	C-C sp ² diff. charged	02	729
		286.2	0.77	1.14	C-O-C, C-Cl	0.08	2,786
		290.9	0.77	1.14	COO, COOH	0.01	290
		292.1	0.77	1.14	π - π^* shake up	0.01	123

TRGO-Trz _L -hPG	C1s	284.6	0.49	0.89	C-C sp ²	0.40	7,364
		284.0	0.49	1.31	C-C sp ² diff. charged	0.01	125
		285.5	0.49	0.89	C-N, C-O-H	0.10	1,934
		286.8	0.49	0.89	C-O-C, O-C-O	0.48	8,835
TRGO-Trz _L -hPG _L -CD	C1s	284.6	0.50	1.32	C-C sp ²	0.34	7,779
		283.9	0.50	0.93	C-C sp ² diff. charged	0.05	1,063
		285.3	0.50	1.32	C-N, C-O-H	0.09	1,956
		286.6	0.50	1.32	C-O-C, O-C-O	0.44	9,857
		288.1	0.50	1.32	COO, COOH	0.08	1746
TRGO-hPG _L	C1s	284.6	0.87	0.92	C-C sp ²	0.68	27,379
		286.6	0.87	1.18	C-O-C, C-O-H	0.20	8,261
		287.1	0.87	1.11	C=O, O-C-O	0.11	4,250
		288.8	0.87	1.11	COO, COOH	0.01	605
TRGO-hPG _H	C1s	284.6	0.73	0.88	C-C sp ²	0.36	11,461
		284.4	0.54	1.2	C-C sp ² diff.charged	0.03	874
		285.7	0.54	1.2	C-N-H	0.12	3,903
		286.9	0.54	1.2	C-O-C, C-O-H	0.32	10,300
		287.5	0.54	1.2	C=O, O-C-O	0.12	3,766
		288.6	0.54	1.2	NH-C=O	0.03	1,006
		289.2	0.54	1.2	COO, COOH	0.01	464
TRGO-L-Cys	C1s	284.6	0.82	0.93	C-C sp ²	0.85	38,698
		285.7	0.79	1.12	C-O-C, C-N-H	0.08	3,551
		286.9	0.79	1.12	C=O, O-C-O	0.03	1,346
		288.2	0.79	1.12	COO, COOH	0.06	1,319
		288.9	0.79	1.12	π-π* shake up	0.02	694
	S2p	163.9	0.44	1.07	C-S-H	0.82	265
		168.4	0	1.07	SO ₂	0.18	60
TRGOL, D-Cys	C1s	284.6	0.81	0.88	C-C sp ²	0.85	31,333
		286.2	0.88	1.09	C-O-C, C-N-H	0.09	3,448
		286.9	0.88	1.09	C=O, O-C-O	0.03	1,244
		288.2	0.88	1.09	COO, COOH	0.02	913
	S2p	164.0	0.23	1.38	C-S-H	0.82	464
		167.7	0	2.75	SO ₂	0.18	99

Table S4. Resonances in the C and N K-edge NEXAFS measured with TRGO, TRGO-Trz and polyglycerol-functionalized-TRGO.

Sample		Photon energy	Assignment	Refs.
C K-edge NEXAFS				
TRGO	d	285.4	C1s \rightarrow π^*	4
		291.8	Excitonic contribution	4
		292.8	C 1s \rightarrow σ^* band-like contributions	4
TRGO-Trz _i (i=1-3)	d ^{''}	285.0	C1s \rightarrow π^*	
	d [']	285.3	C1s \rightarrow π^*	
	d	285.4	C1s \rightarrow π^* (TRGO)	4
	e	287.2	C 1s \rightarrow σ^*_{C-N}	9
	f	288.1	C 1s \rightarrow σ^*_{C-N} , C1s \rightarrow $\pi^*_{C=N}$	9
	g	289.3	C 1s \rightarrow σ^*_{C-N}	9
		291.8	Excitonic contribution (TRGO)	4
		292.9	C 1s \rightarrow σ^* band-like contributions (TRGO)	4
TRGO-hPG _L TRGO-hPG _H	j	285.4	C1s \rightarrow π^* (TRGO)	4
	k	286.3		
	l	287.2		
	m	288.1		
	n	289.4	C-H*	4
N K-edge NEXAFS				
TRGO-Trz _i (i=1-3)	h	399.4	N1s \rightarrow π^* (triazine ring)	18,19

	i	400.6		
TRGO-hPG _L	o'	398.8		
	o	399.4	N1s → π* (triazine ring)	18,19
	q	400.6		
	r	401.3		
TRGO-hPG _H	o'	398.8		
	o	399.4	N1s → π* (triazine ring)	18,19
	p	399.8		
	q	400.6		
	r	401.3	N1s → π* (amine)	23
	s	401.8		

There are no one-by-one reference C K-edge spectra in the literature for triazine bound to graphene but a spectrum of a complex LB film made of a 2-vinyl-4,6 diamino s triazine /2-(perfluorodecyl)ethyl acrylate co-polymer had been published displaying a C1s → π*_{C=N} resonance at 288.6 eV¹⁹ [ENREF 7](#)¹ what is near to resonance (f) in our experiment. However, the bonding situation for triazine is rather different in both cases. In this context it is remarkable that in C K-edge spectra the evolution of π* resonances (d' and d'') was observed at lower photon energies as for pristine TRGO in correlation to increasing triazine attachment on TRGO.

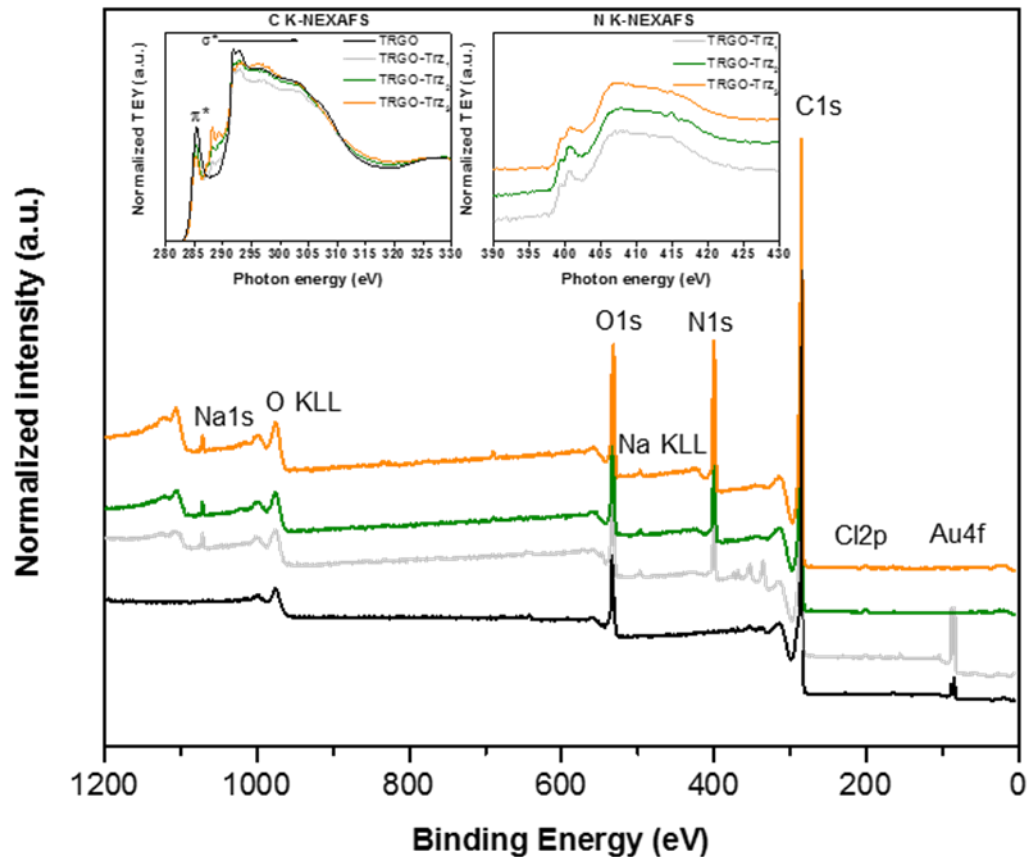


Figure S3. Survey XPS spectra of pristine TRGO (black) and different runs TRGO-Trz showing oxygen, carbon, nitrogen, and chlorine. C K-edge and N K-edge NEXAFS spectra of TRGO, TRGO-Trz₁, TRGO-Trz₂ and TRGO-Trz₃.

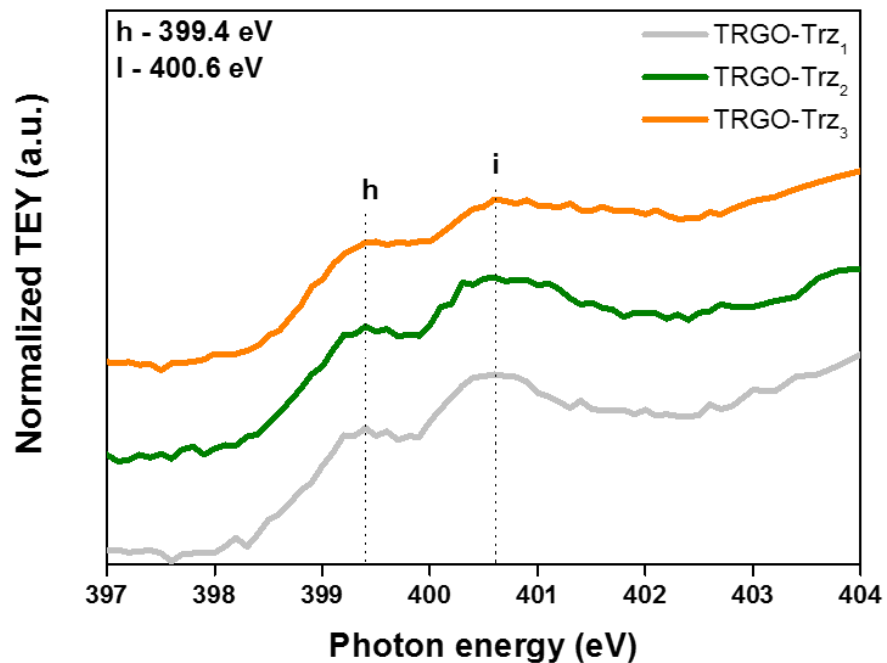


Figure S4. Expanded low energy section of N K-edge NEXAFS of TRGO-Trz₁, TRGO-Trz₂ and TRGO-Trz₃. The N K-edge spectra reveal two sharp resonances (h, i) which are related to the dichlorotriazine group and its N atom linked to TRGO.^[10,11] For full NEXAFS spectra and assignments see Figure S3 and Table S4.

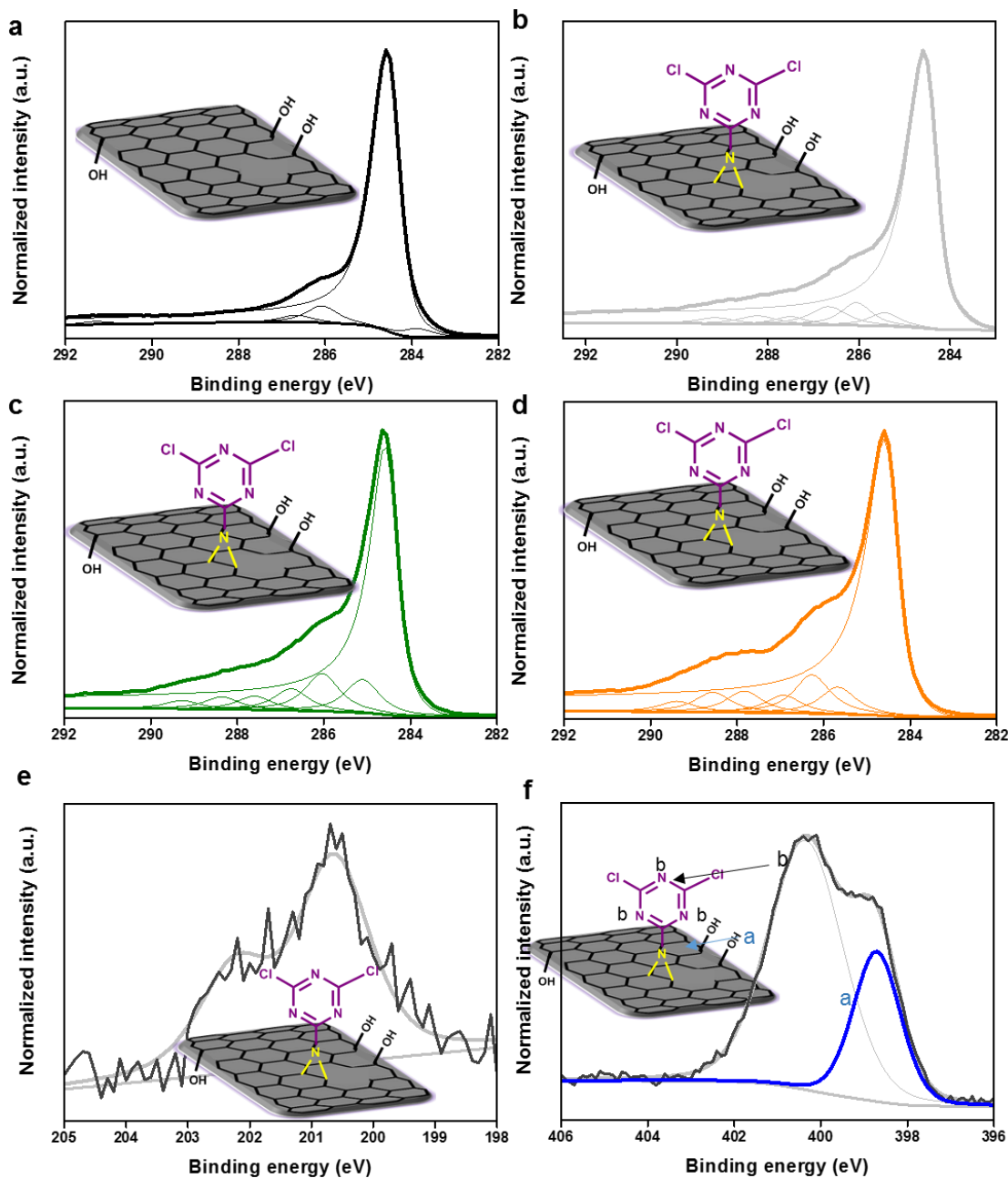


Figure S5. Highly resolved XPS spectra with peak fitting for **a**, C1s TRGO, **b**, C1s TRGO-Trz₁, **c**, C1s TRGO-Trz₂, **d**, C1s TRGO-Trz₃ and **e**, Cl2p TRGO-Trz₁, **f**, highly resolved N1s XPS spectra of TRGO-Trz₁. All binding energies (BE) are in the range of nitrogen atoms with sp² hybridization.^[12] The highly resolved N1s XPS spectrum shows two component peaks at BE 398.7 and 400.4 eV which are assigned as (a) and (b) corresponding to the structure of the dichlorotriazine groups on the surface of TRGO (Figure S5f).^[13] The peak at 400.4 eV is assigned to the nitrogen atoms in the triazine rings.^[12,14-16] The Cl2p_{3/2} peak at 200.6 eV is

assigned to chlorine atoms in dichlorotriazine which are important for controlled post-modification of TRGO-Trz^[17] (figure S5e). A ring related C1s $\rightarrow \pi^*_{C=N}$ resonance has to be expected for the conjugated dichlorotriazine groups, but it might be superimposed with TRGO π^* features.^[18,19,9] Fit parameters for each spectra are shown in Table S3.

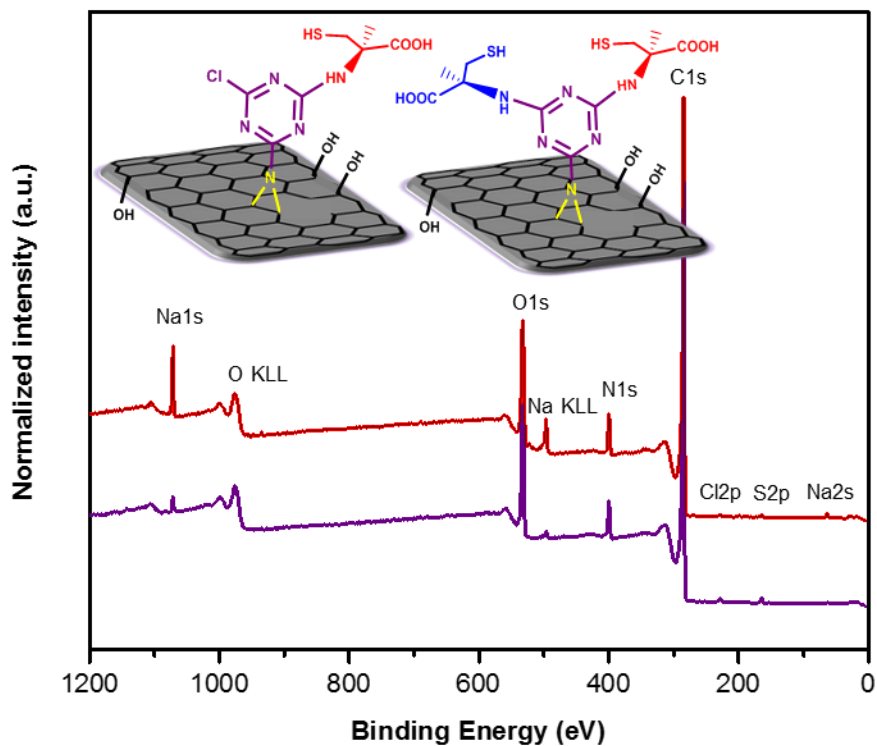


Figure S6. Survey XPS spectra of TRGO-L-Cys (red) and TRGO-L, D-Cys (purple) show oxygen, nitrogen, carbon, and sulfur.

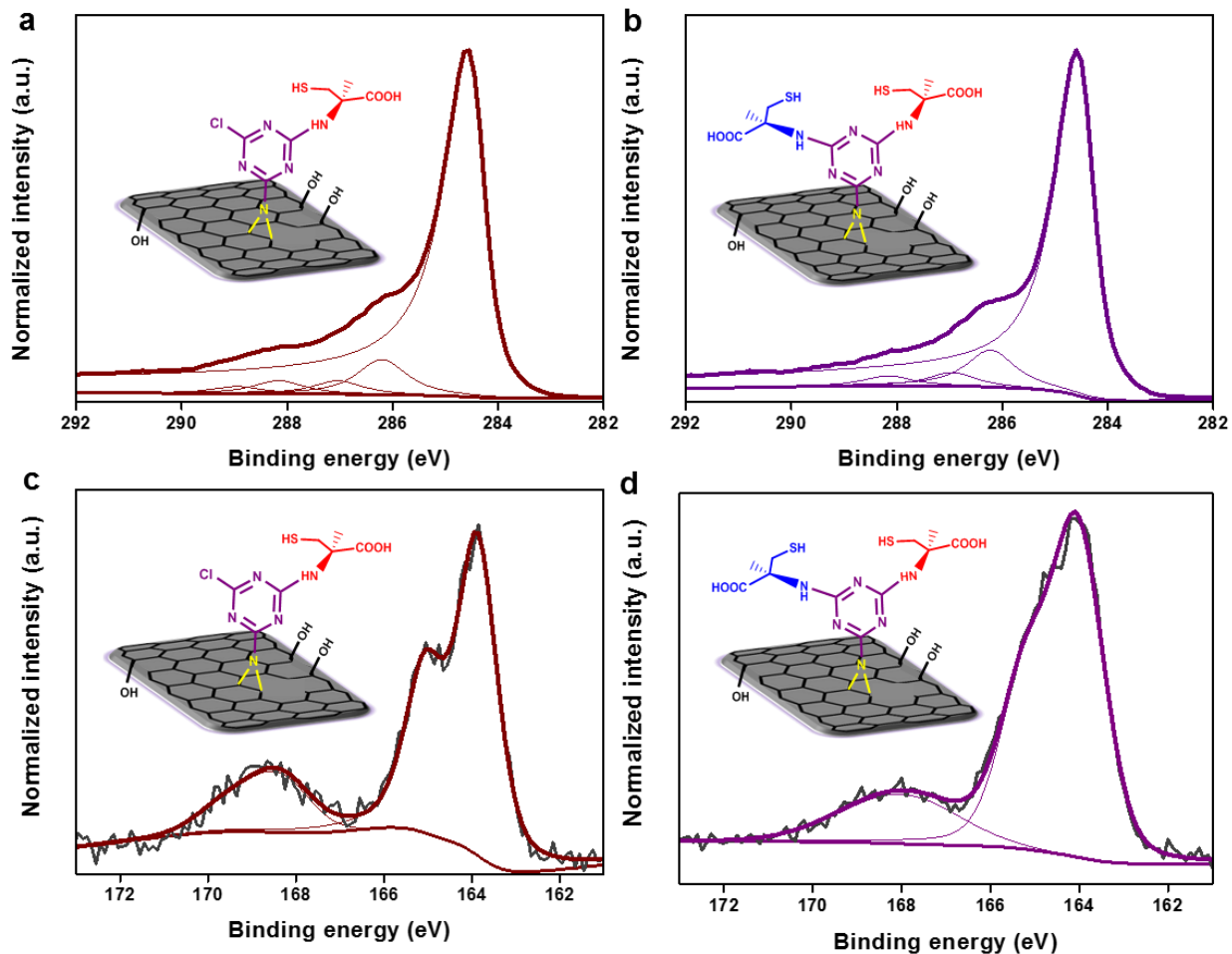


Figure S7. Highly resolved S2p and C1s XPS spectra of TRGO-L-Cys and TRGO-L, D-Cys. **a**, C1s TRGO-L-Cys, **b**, C1s TRGO-L, D-Cys, **c**, S2p TRGO-L-Cys, and **d**, S2p TRGO-L, D-Cys. Unresolved doublet at around BE = 169 eV is assigned to the oxidation of a part of thiol groups to sulfoxide.^{[20 [ENREF 8](#)]} Consistent with IR spectroscopy and elemental analysis, the S2p_{3/2} peak at 163.9 eV in the XPS spectra of TRGO-L-Cys and TRGO-L, D-Cys confirms the conjugation of cysteine to TRGO (S7c,d). Furthermore, the sulfur/carbon (S/C) peak area ratio in the XPS survey spectra of TRGO-L-Cys and TRGO-L, D-Cys is 0.007 and 0.015, respectively. The increase in S/C ratio is very close to the optimal yield, assuming it doubles after the second reaction step. These results further support a controlled, consecutive conjugation of L- and D-cysteine to the surface of TRGO. Fit parameters for each spectra are shown in Table S3.

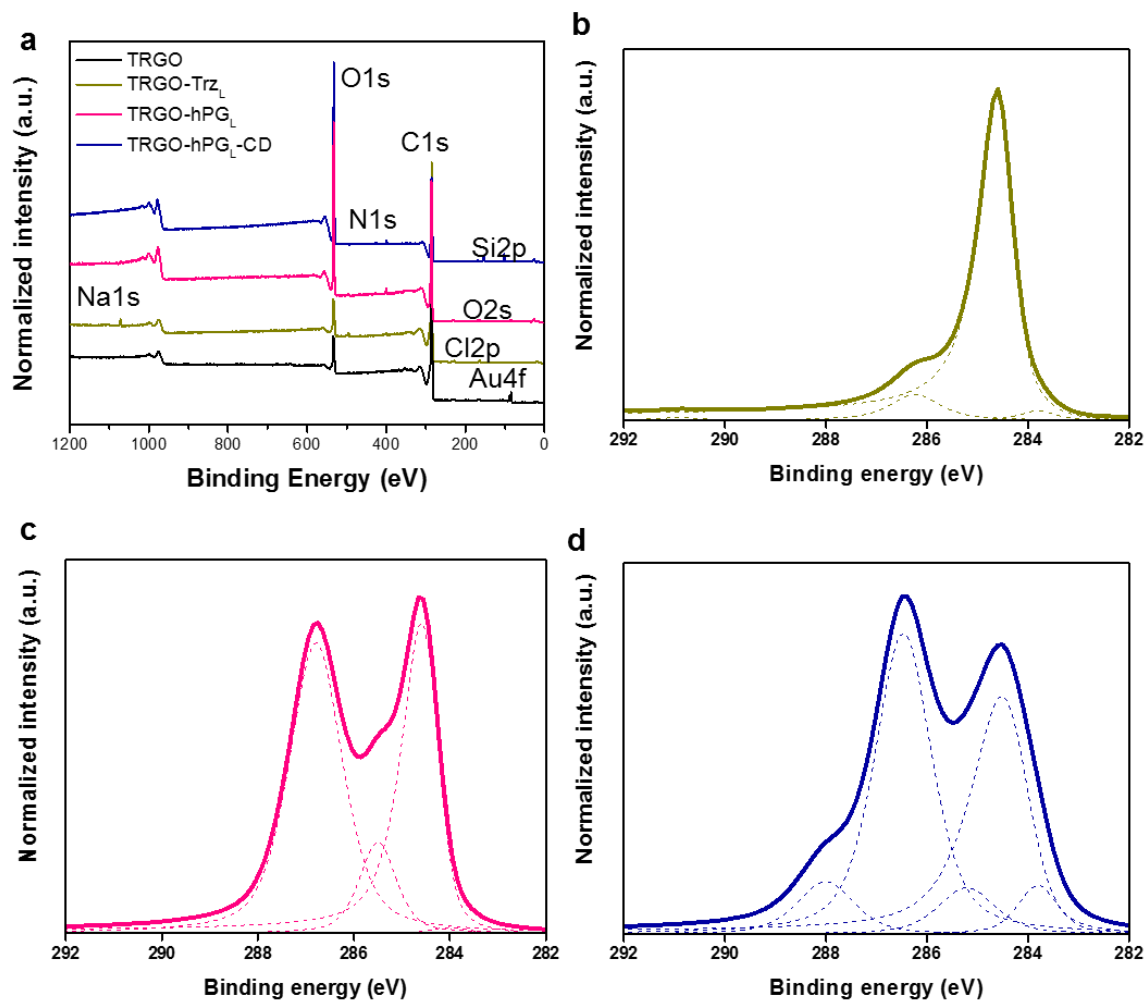


Figure S8. a) Survey spectra of TRGO, TRGO-Trz_L, TRGO-hPGL and TRGO-hPGL-CD. Stepwise conjugation of PG and β CD to the surface of TRGO-Trz_L increased oxygen content from 7.9% to 19.6 and 28.9% respectively. b-d) highly resolved C1s spectra of TRGO-Trz_L, TRGO-hPGL and TRGO-hPGL-CD, respectively. Change in the spectra is due to the chemical modification of the surface. Increase in the ratio of TRGO to PG/PGL- β CD from 1.4 to 1.5 proves conjugation of β CD to the surface of TRGO-Trz_L. Hence, XPS proves successful covalent conjugation of both PG and β CD to the surface of TRGO-Trz_L.

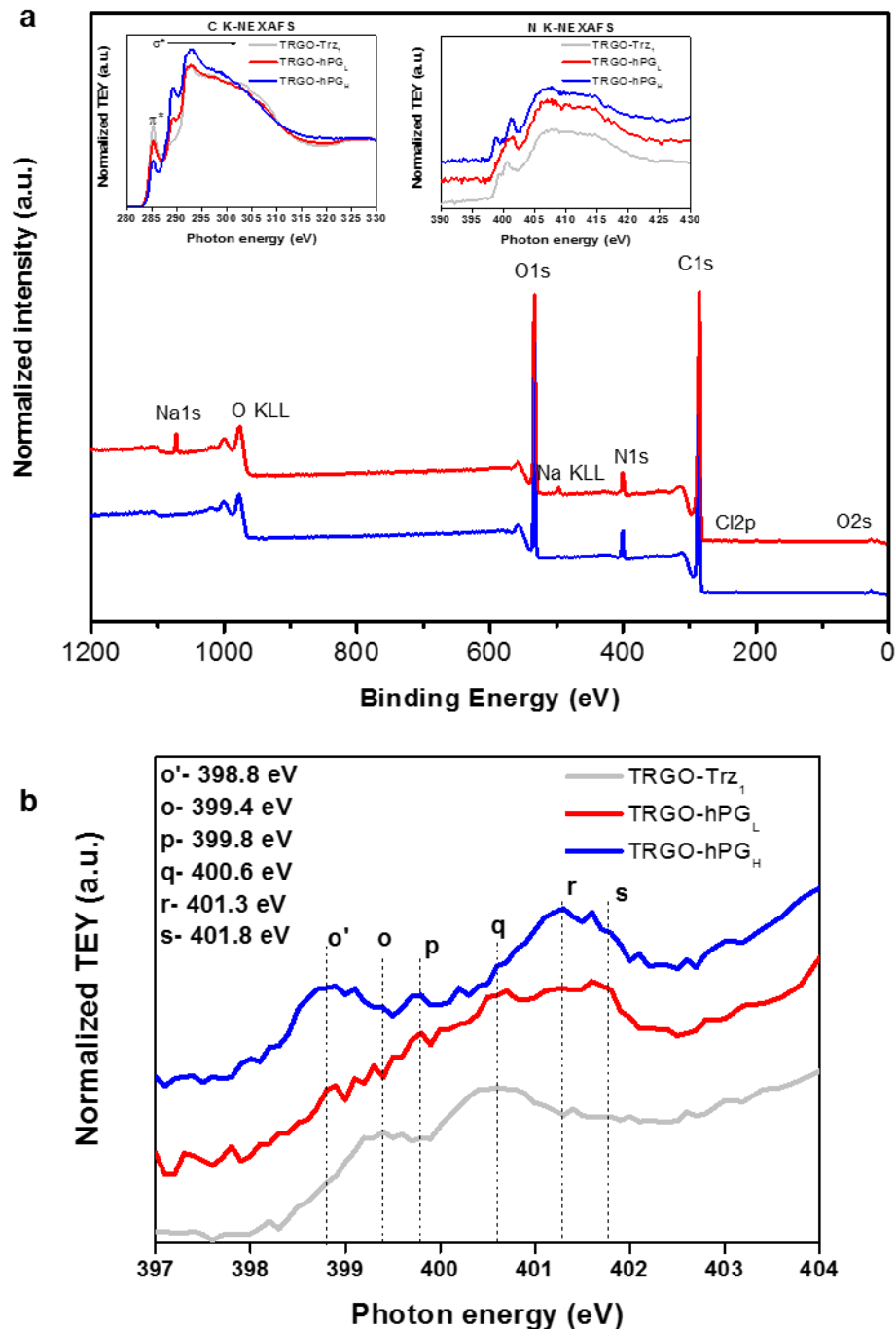


Figure S9. a, survey XPS spectra, N K-edge and C K-edge NEXAFS of TRGO-Trz, TRGO-hPG_L (red) and TRGO-hPG_H (blue). **b**, Expanded low energy section of N K-edge NEXAFS of TRGO-hPG_L and TRGO-hPG_H. For assignments see the Supplementary Table 4. In N K-edge NEXAFS the most intense N1s $\rightarrow \pi^*$ resonance for triazole occurs at 400.3 eV^[21,22]. Furthermore a N1s $\rightarrow \pi^*$ resonance of amines above 401 eV^[23] is expected. In the experimental spectra, π^*

resonances (o, o') at lower energies compared to TRGO-Trz are detected. A wider range of new resonances occurs after reaction of polyglycerol azide with TRGO-Trz. The clearest result in N K-edge NEXAFS is the resonance assigned to amine bonds, providing proof of successful conjugation of hPG-NH₂ to TRGO-hPG_L. The C_{hPG}/C_{TRGO} ratio increased from 0.46 to 1.23 upon nucleophilic substitution of the second chlorine atom of dichlorotriazine groups by polyglycerol amine. From this ratio, the calculated polymer content for TRGO-hPG_H was ~55 wt.%, which is similar to the values ~58 wt.% obtained by TGA (Figure S15b).

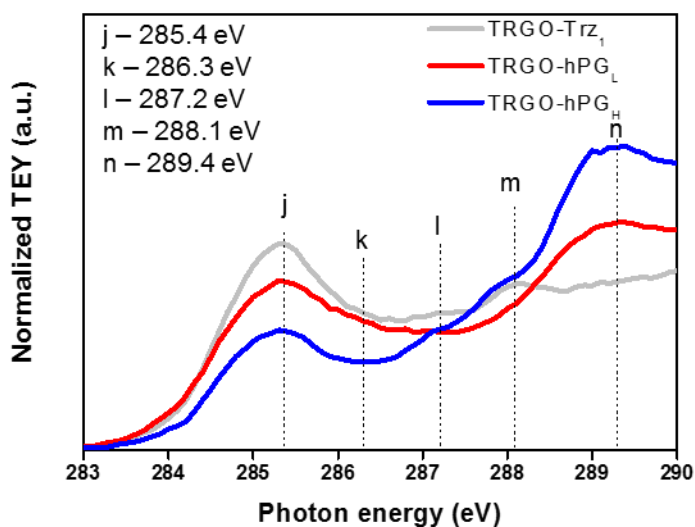


Figure S10. Expanded low energy section of C K-edge NEXAFS of TRGO-Trz before and after reaction with hPG derivatives.

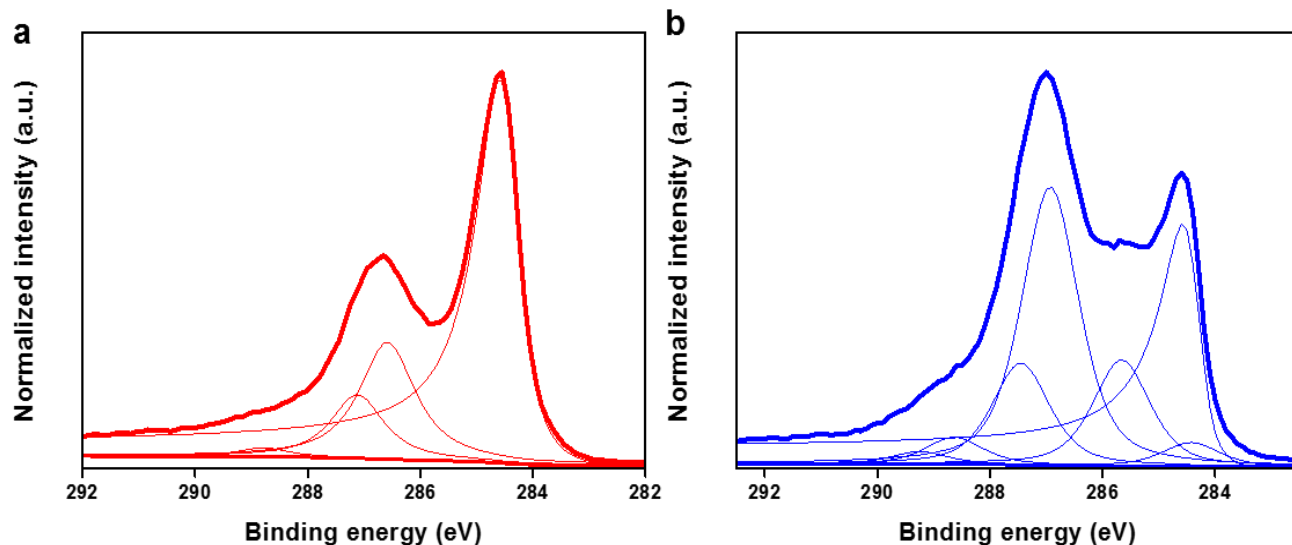


Figure S11. Highly resolved XPS spectra with peak fitting for **a**, C1s TRGO-hPGL (red), **b**, C1s TRGO-hPGH (blue). Fit parameters for each spectra are shown in Table S3. In the XPS spectra of TRGO-hPGL and TRGO-hPGH, an intense peak in the BE range 286.3 to 287.3 eV is assigned to the backbone (C–O) of hPG. Other C1s component peaks relate to TRGO as described above, indicating conjugation of hPG onto TRGO-Trz₁.

Loading capacity:

Figure 3b in the main text shows the UV spectra of free rhodamine 6G and the same spectra when it is loaded on TRGO-hPGL-CD and TRGO-hPGL. An aqueous solution of rhodamine 6G (5 mL, 0.1 μ M) was added to a dispersion of the functionalized graphene sheets (5 mL, 1 mg/mL) at room temperature and mixture was stirred for 30 minutes. Then mixtures were centrifuged (6000 rpm, 20 minutes) and graphene sheets were precipitated. The loading capacity of graphene sheets was then calculated according to the following equation and using a calibration curve. The ratio of loading capacity of TRGO-hPGL-CD to TRGO-hPGL was calculated to be 1.6, respectively.

$$\text{Loading capacity} = \frac{\text{Weight of loaded guest molecule}}{\text{Weight of carrier} + \text{weight of loaded guest molecule}} \times 100$$

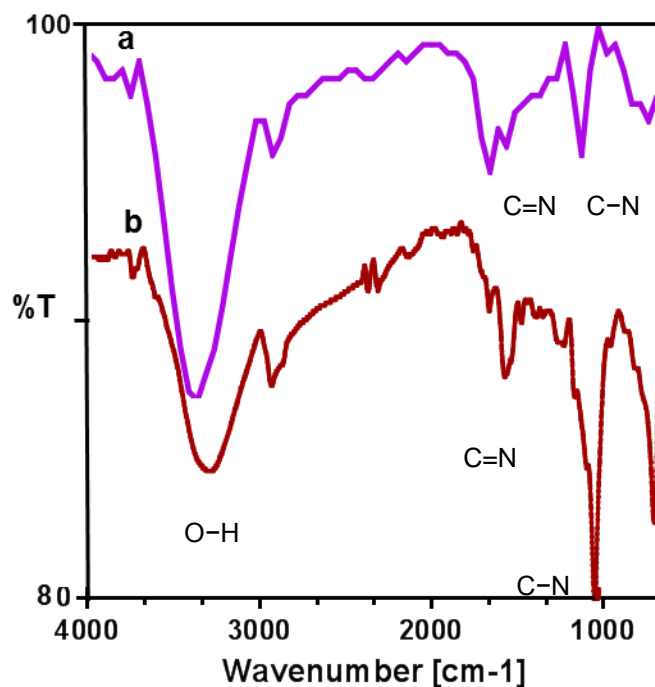


Figure S12. IR spectra of a) TRGO-hPGL and b) TRGO-hPGL-CD.

Figure S12 shows the IR spectra of TRGO-hPGL and TRGO-hPGL-CD. As it can be seen, after conjugation of cyclodextrin to TRGO-hPGL, the intensity of the absorbance band at 1030 cm⁻¹ is increased. This band is assigned to the C–O bonds of cyclodextrin and therefore proves conjugation of cyclodextrin to the graphene sheet.

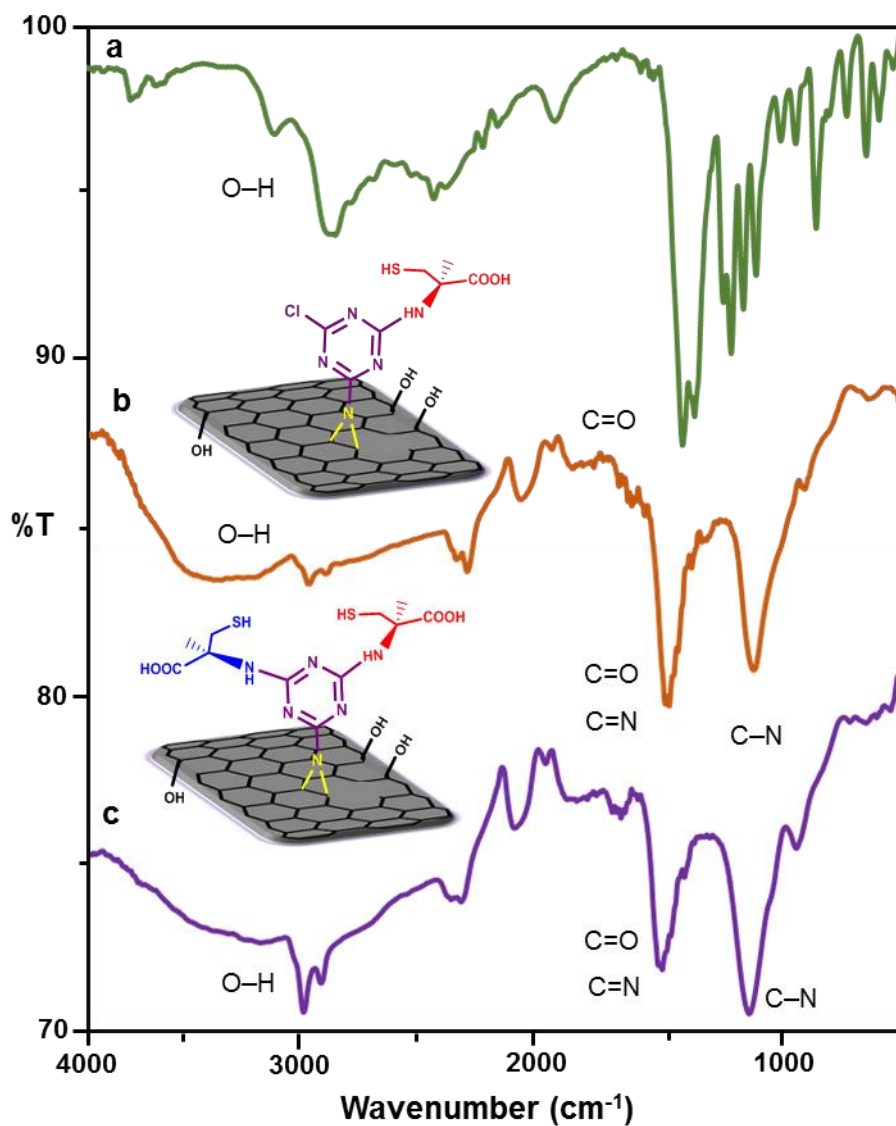


Figure S13. IR spectra of **a**, L-Cysteine, **b**, TRGO-L-Cys and **c**, TRGO-L, D-Cys. A broad absorbance band at 1,637 and 1,562 cm⁻¹ is assigned to the carbonyl group of amino acids and C=N bonds of dichlorotriazine groups. The absorbance band of the hydroxyl group of amino acids at 3,473 and 2,822 cm⁻¹ indicates conjugation of cysteine to the surface of TRGO-Trz₁.

Table S5. Nitrogen, carbon, hydrogen and sulfur content of TRGO-L-Cys and TRGO-L, D-Cys measured by elemental analysis.

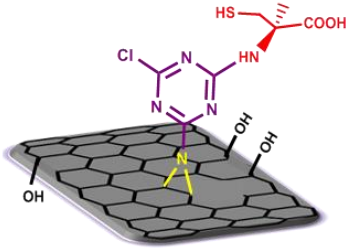
Compound	N%	C%	H%	S%	Cys%
TRGO-Trz ₁	7.30	76.26	2.73	-	-
TRGO-L-Cys	8.77	65.58	2.92	3.90	1:47
TRGO-L, D-Cys	11.15	66.99	3.45	6.19	1:22

Elemental analysis shows a sulfur content of ~3.90 wt.% and ~6.19 wt.% for TRGO-L-Cys and TRGO-L, D-Cys, respectively. This proves stepwise conjugation of L- and D-cysteine to TRGO-Trz₁.

Calculation of DF of cysteine group

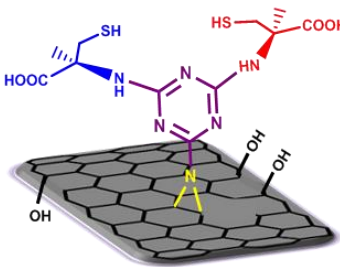
Calculation of the number of cysteine molecules conjugated to TRGO-Trz₁ at 25 °C and 60 °C based on S (wt.%) content as following:

X	32	(Mass of S atom of one triazine-cysteine group)	at 25 °C
100	3.9		
X = 820.51 (Mass of building block of TRGO-L-Cys)			
820.51 – 248 = 572.51			
DF = 572.51/12 = 47.7			
248 is mass of triazine + cysteine group			



TRGO-L-Cys

X	32	(Mass of S atom of one triazine-cysteine group)	at 60 °C
100	6.2		
X = 516.12 (Mass of building block of TRGO-L, D-Cys)			
516.12 – 248 = 268.12			
DF = 268.12/12 = 22.3			
248 is mass of triazine + cysteine group			



TRGO-L, D-Cys

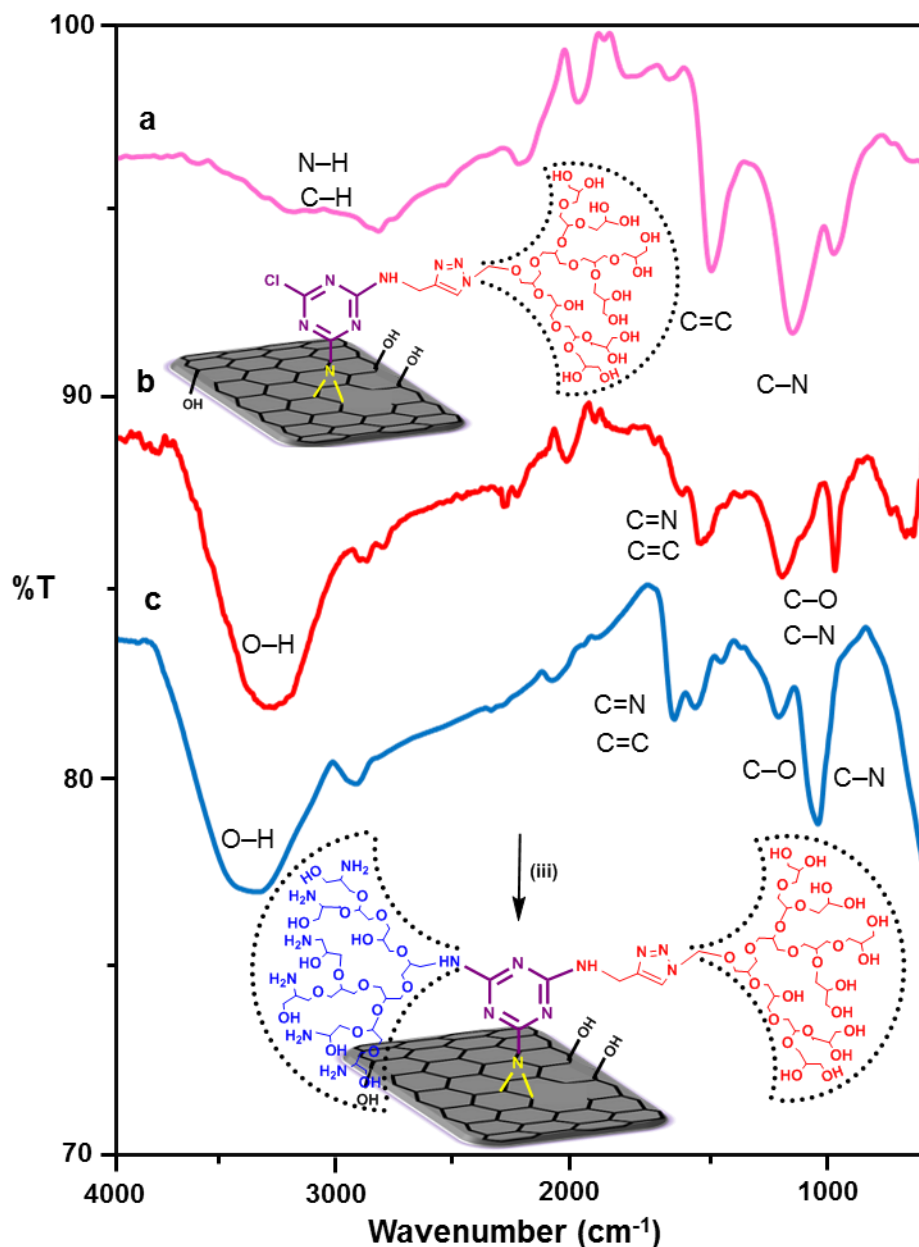


Figure S14. IR spectra of the, **a**, TRGO-propargyl, **b**, TRGO-hPGL and **c**, TRGO-hPGH. In the IR spectra of propargylamine-functionalized TRGO, absorbance bands of N–H and C–H bonds of propargylamine appear at 3,308 and 2,925 cm⁻¹, respectively. (b) and (c) absorbance bands of C=C (TRGO), C=N (triazine and triazole rings) and C–N (triazine and triazole rings and also polyglycerol) bonds can be observed at 1,642, 1,530 and 1,185 cm⁻¹, respectively. Strong absorbance bands at 3,350 and 1,120 cm⁻¹ are assigned to the O–H and C–O bonds of polyglycerol.

Calculation of number of propargylamine groups:

$(50 \times 12) + 163.5 + 55 - 35.5 - 1 = 782$ (Mass of a building block of propargylamine-functionalized TRGO-Trz₁)

In an optimum functionalization at room temperature one of the chlorine atoms of all of triazine groups should be substituted by propargylamine and therefore nitrogen content of the product should be:

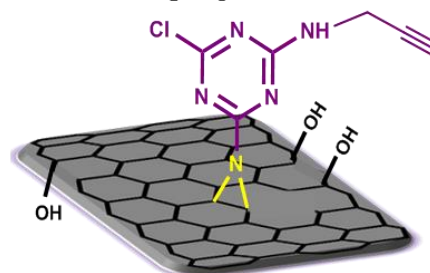
782 (5 × 14) (5 is the number of N atoms of triazine-propargylamine groups)

100 X X = 8.9

Since the nitrogen content of the product is 8.3, around 93% of the triazine groups onto the surface of TRGO-Trz₁ are functionalized by propargylamine.

100 8.9

X 8.3 X = 93%



TRGO-propargyl

Calculation of the number of propargylamine molecules conjugated to TRGO-Trz₁ based on N (wt.%) content (elemental analysis) as following: Elemental analysis shows an increase in the nitrogen content from 7.0 wt.% to 8.3 wt.% after the reaction of TRGO-Trz₁ with propargylamine. This is in accordance with the substitution of one chlorine atom from each dichlorotriazine group by propargylamine.

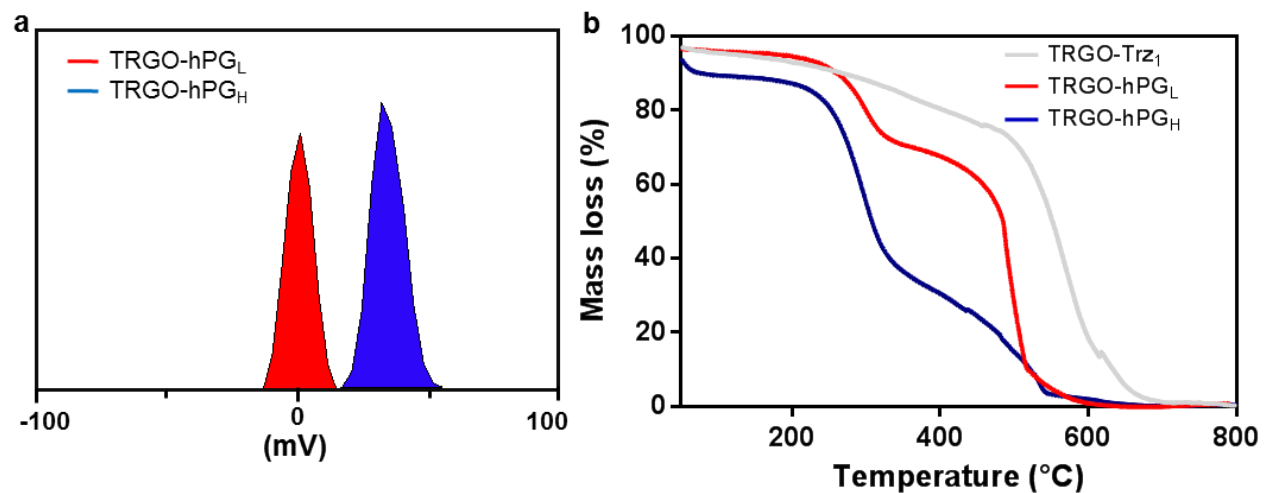


Figure S15. **a**, zeta potential of TRGO-hPGL (red) and TRGO-hPGH (blue) in aqueous neutral solution (pH = 7). Concentrations: 0.1 mg/mL at 25 °C and **b**, TGA thermograms TRGO-Trz₁, TRGO-hPGL and TRGO-hPGH.

Thickness measurements of the TRGO and TRGO-Trz₁:

The thickness of the TRGO and TRGO-Trz₁ sheets were measured and they were found to be 0.9 ± 0.3 nm and 2.2 ± 0.5 nm (error is standard deviation), respectively.

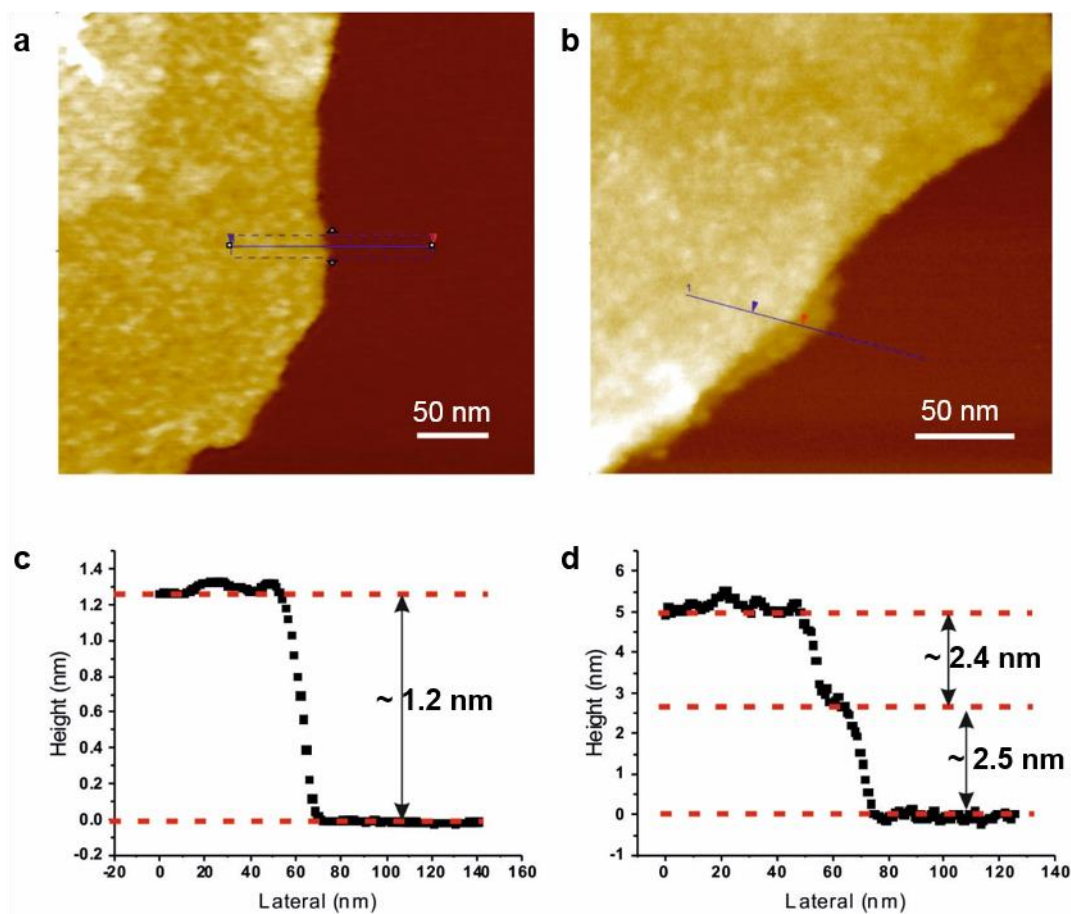


Figure S16. **a**, QNM height image of TRGO from chloroform dispersion as deposited onto HOPG. **b**, QNM height image of TRGO-Trz₁ from chloroform dispersion as deposited onto HOPG. **c**, The profile of the TRGO sheet over HOPG (the blue line in image a). **d**, The profile of the TRGO-Trz₁ sheet over HOPG (the blue line in image b).

Roughness measurements of the TRGO and TRGO-Trz₁:

Roughness measurements for TRGO and TRGO-Trz₁ were carried out in order to determine the triazine homogeneity by scanning the surface of those sheets using SFM in tapping mode. Height histograms of TRGO and TRGO-Trz₁ surfaces were plotted and their root mean square roughness (R_q) was extracted. TRGO and TRGO-Trz₁ were deposited from their dispersions in chloroform onto freshly cleaved surfaces of mica. Roughness analyses were carried out first by analyzing the roughness of the freshly cleaved atomically flat mica surface as a reference for instrumental noise. The root mean square (RMS) roughness value of a mica surface was found to be ~ 0.023 nm to 0.030 nm (Figure S16). Later, TRGO and TRGO-Trz₁ roughnesses were analyzed by scanning a surface area of $0.01\mu\text{m}^2$ of them at 1% relative humidity and at room temperature ($23.5 - 25$ °C). The relative humidity was controlled by placing the SFM, the sample and a humidity sensor (testo 625 – Thermohygrometer with $\pm 2.5\%$ RH accuracy) inside a chamber purged by nitrogen gas. The height histograms of the $0.01\mu\text{m}^2$ surface area over TRGO and TRGO-Trz₁ were plotted and the RMS roughness of them was extracted (Figure S16). The measured R_q for TRGO and TRGO-Trz₁ showed mean values of 0.1 nm and 0.2 nm, respectively (Figure S16). The surface roughness of the TRGO-Trz₁ was found to be higher than that of the TRGO by 0.1 nm which suggests high density packing of triazine groups over TRGO. The higher thickness of TRGO-Trz₁ in comparison to the reported values for TRGO^[24-26] is attributed to the triazine molecules conjugated to both sides. Topography images were processed to reduce vertical drift and were fitted with zero or first order polynomials.

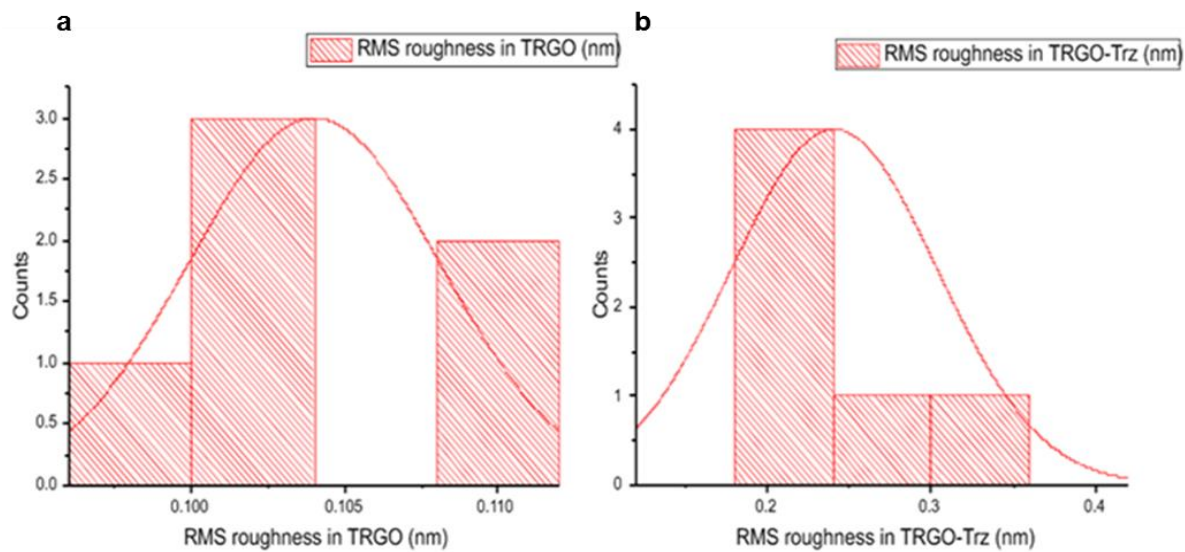


Figure S17. a, Histogram of the RMS roughness values of TRGO deposited onto freshly cleaved mica from chloroform dispersion. **b**, Histogram of the RMS roughness values of TRGO-Trz₁ deposited onto freshly cleaved mica from chloroform dispersion.

Thickness measurements of the TRGO-hPGL and TRGO-hPGH:

The thicknesses of the TRGO-hPGL and TRGO-hPGH sheets were measured using scanning force microscopy in tapping mode. The height histograms of the images (Figure 4b,c in main text and figure S16) were fitted with two Gaussian functions and the difference between the mean values of the fits was assumed to be the sheets heights (See main text for more discussion)

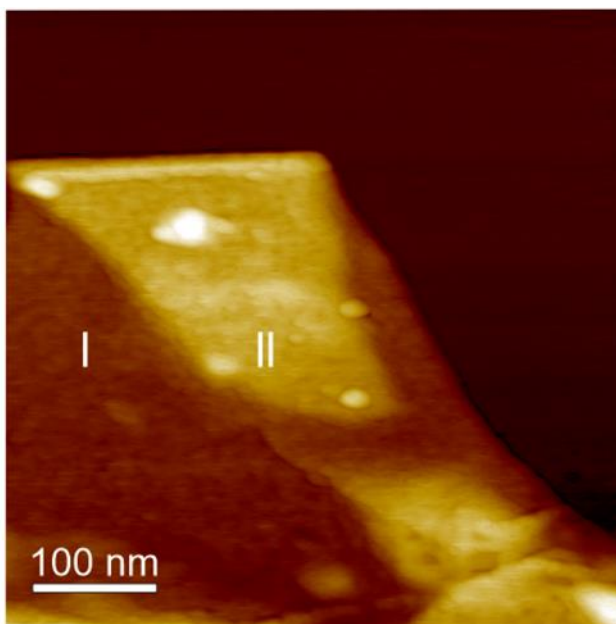


Figure S18. AFM image of the TRGO-hPGH. The area of single (I) and double (II) layered fitted with Gaussian functions. See figure 4c in the main text for height histogram.

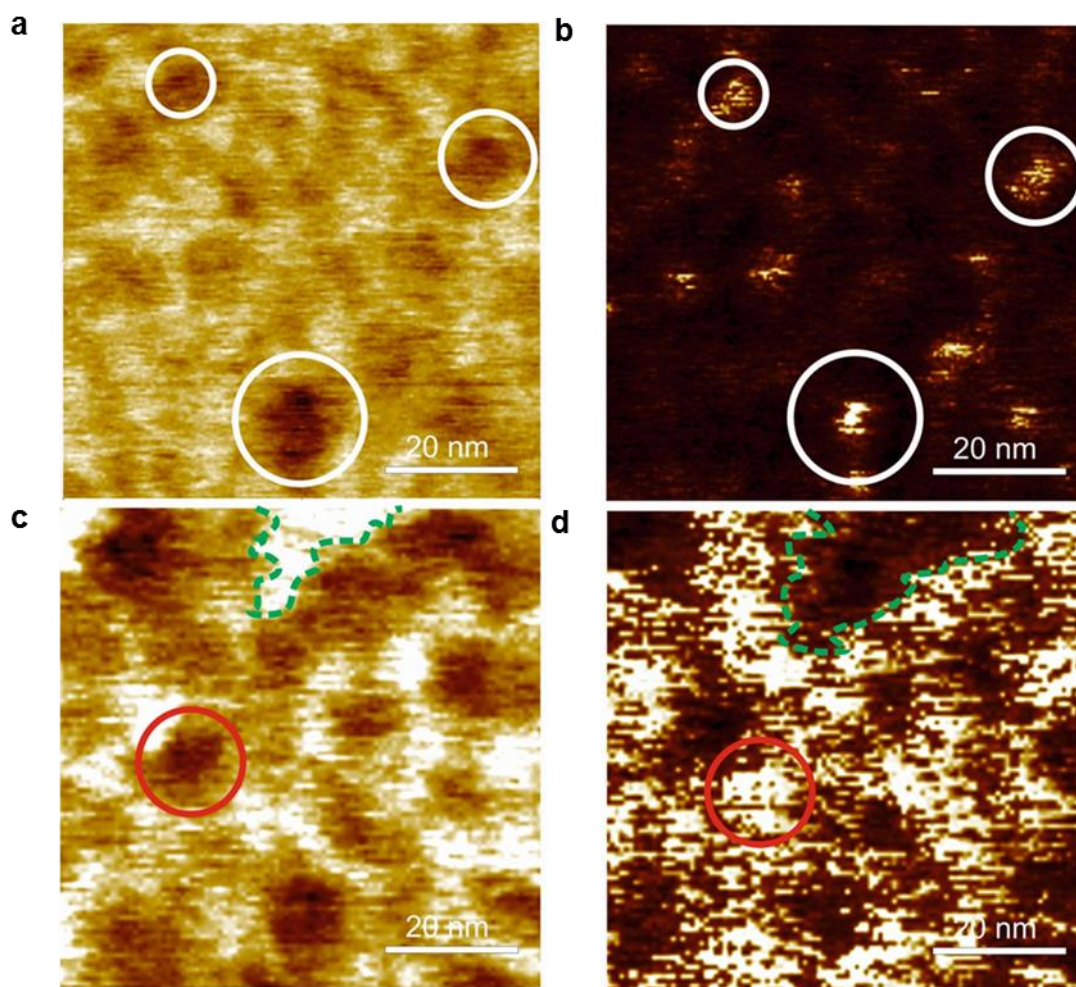
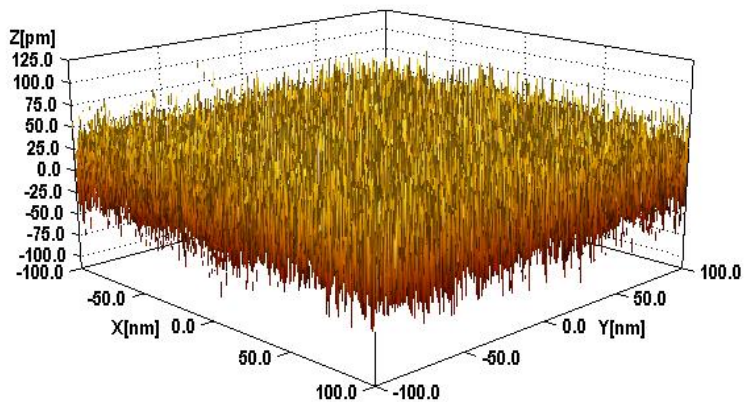


Figure S19. **a**, QNM-SFM pull off force image of TRGO-hPG_L. **b**, Deformation image of the TRGO-hPG_L from the same area as the (a) white circles show hyperbrach polyglycerol (hPG) locations in (a, b). **c**, QNM-SFM pull of force image of TRGO-hPG_H. **d**, Deformation image of the TRGO-hPG_H from the same area as the (c) red circle shows hyperbrach polyglycerol hPG location in (c and d), green dotted line shows the proximity with higher adhesion in (c) and lowest deformation in (d) low deformation is attributed to the higher TRGO hardness in compare to hPG. Scale for a, b, c and d is 20 nm.

a



b

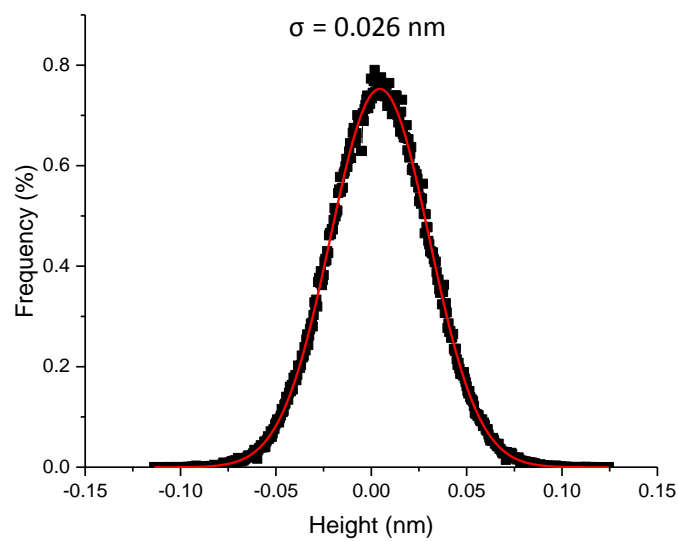


Figure S20. TM-SFM roughness analysis of the mica surface **a**, 3D view of the height variations over freshly cleaved mica. **b**, Histogram of the height data extracted from image (a). Sigma shows the RMS surface roughness to be $\sim 0.026 \text{ nm}$.

Stereoscopic image of TRGO-hPG_H

Since polyglycerol amines are positively charged, the ability of TRGO-hPG_H to load negatively charged gold nanoparticles (AuNPs) by electrostatic interactions was studied. Neutral TRGO-hPG_L was used as a control with AuNPs (Figure S15a). The Cryo-TEM images show that both TRGO-hPG_L and TRGO-hPG_H can be dispersed in aqueous solutions, confirming the hydrophilicity of polyglycerol coated TRGO.

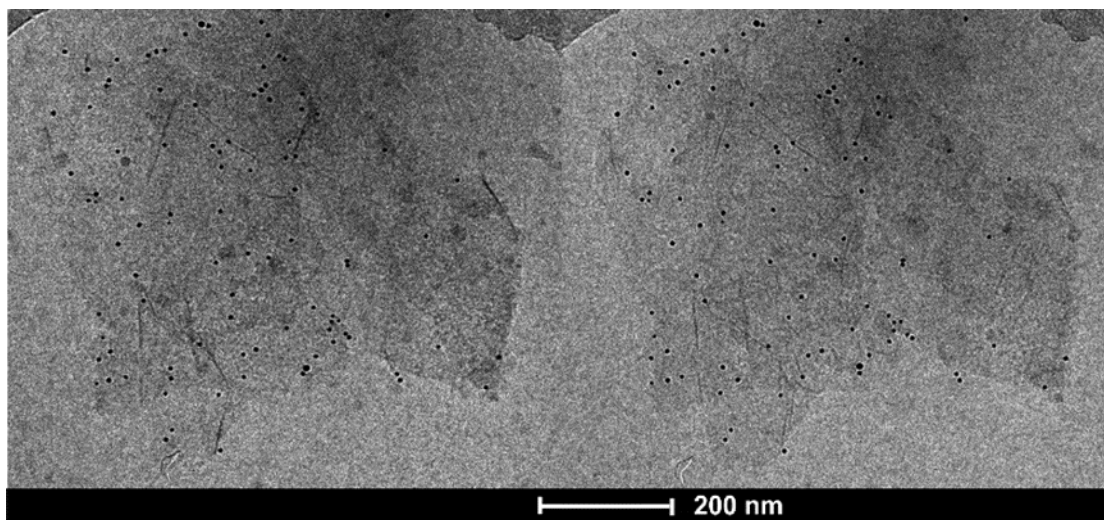


Figure S21. The stereo image of TRGO-hPG_H with gold nanoparticles which attached the surface of hyperbranched polyglycerol amine by electrostatic interaction.

References

- [1] B. Schlüter, R. Mülhaupt, A. Kailer, *TRIBOL. LETT*, **2013**, 53, 353-363.
- [2] K. Heister, M. Zharnikov, M. Grunze, L. S. O. Johansson, A. Ulman, *Langmuir*, **2001**, 17, 8-11.
- [3] Stöhr, J. *Principles, Techniques, and Instrumentation of NEXAFS*, (Springer Berlin Heidelberg: Berlin, Heidelberg, 1992).
- [4] P. E. Batson, *Phys. Rev. B*, **1993**, 48, 2608-2610.
- [5] S. Roller, H. Zhou, R. Haag, *Molec. Divers*, **2005**, 9, 305-316.
- [6] P. Ofek, W. Fischer, M. Calderón, R. Haag, R. Satchi-Fainaro, *FASEB J.* **2010**, 24, 3122-3134.
- [7] N. Ito, N. Yoshida, K. Ichikawa, *J. Chem. Soc Perkin Trans*, **1996**, 2, 965–972.
- [8] C.Y. Quan, J.X. Chen, H.Y. Wang, C. Li, C. Chang, X.Z. Zhang, R.X. Zhuo, *ACS NANO*, **2010**, 4, 4211–4219.
- [9] A. Fujimori, N. Sato, K. Kanai, Y. Ouchi, K. Seki, *Langmuir*, **2009**, 25, 1112-1121.
- [10] G. Vall-Ilosera, B. Gao, A. Kivimäki, M. Coreno, J. Álvarez Ruiz, M. d. Simone, H. Agren, E. Rachtew, *J. Chem. Phys*, **2008**, 128, 139901.

- [11] G. M. Whitesides, E. E. Simanek, J. P. Mathias, C. T. Seto, D. Chin, M. Mammen, D. M. Gordon, *Acc. Chem. Res.*, **1995**, 28, 37-44.
- [12] W. J. Gammon, O. Kraft, A. C. Reilly, B. C. Holloway, *Carbon*, **2003**, 41, 1917-1923.
- [13] B. Yuan, C. Bao, L. Song, N. Hong, K. M. Liew, Y. Hu, *Chem. Eng. J.*, **2014**, 237, 411-420.
- [14] G. A. Siller, N. Severin, S. Y. Chong, T. Björkman, R. G. Palgrave, A. Laybourn, M. Antonietti, Y. Z. Khimyak, A. V. Krashennnikov, J. P. Rabe, U. Kaiser, A. I. Cooper, A. Thomas, M. J. Bojdys, *Angew. Chem. Int. Ed.*, **2014**, 53, 7450-7455.
- [15] D. Deng, X. Pan, L. Yu, Y. Cui, Y. Jiang, J. Qi, W. X. Li, Q. Fu, X. Ma, Q. Xue, G. Sun, X. Bao. *Chem. Mater.*, **2011**, 23, 1188-1193.
- [16] L. G. Bulusheva, A. V. Okotrub, Y. V. Fedoseeva, A. G. Kurenya, I. P. Asanov, O. Y. Vilkov, A. A. Koós and N. Grobert, *Phys. Chem. Phys.*, **2015**, 17, 23741-23747.
- [17] A. R. Silva, C. Freire, B. de Castro, M. M. M. Freitas, J. L. Figueiredo, *Microporous Mesoporous Mater.*, **2001**, 46, 211-221.
- [18] E. Apen, A. P. Hitchcock, J. L. J. Gland, *Phys. Chem.*, **1993**, 97, 6859- 6866.
- [19] G. Vall-Ilosera, B. Gao, A. Kivimäki, M. Coreno, J. Álvarez Ruiz, M. de Simone, H. Agren, E. Rachlew, *J. Chem. Phys.*, **2008**, 128, 139901.
- [20] B. J. Lindberg, K. Hamrin, G. Johnsson, U. Gelius, A. Fahlman, K. Siegbahn, *Phys. Scr.*, **1970**, 1, 286-289.
- [21] E. Darlatt, A. Nefedov, C. H.-H. Traulsen, J. Poppenberg, S. Richter, P. M. Dietrich, A. Lippitz, R. Illgen, J. Kühn, C. A. Schalley, C. Wöll, W. E. S. Unger, *J. Electron. Spectrosc. Relat. Phenom.*, **2012**, 185, 621-624.
- [22] D. Deng, X. Pan, L. Yu, Y. Cui, Y. Jiang, J. Qi, W. X. Li, Q. Fu, X. Ma, Q. Xue, G. Sun, X. Bao. *Chem. Mater.*, **2011**, 23, 1188-1193.
- [23] N. Graf, E. Yegen, T. Gross, A. Lippitz, W. Weigel, S. Krakert, A. Terfort, W. E.S. Unger. *Surf. Sci.*, **2009**, 603, 2849-2860.
- [24] I. Jung, M. Vaupel, M. Pelton, R. Piner, D. A. Dikin, S. Stankovich, J. An R. S. Ruoff, *J. Phys. Chem. C*, **2008**, 112, 8499-8506.
- [25] E. Apen, A. P. Hitchcock, J. L. J. Gland, *Phys. Chem.*, **1993**, 97, 6859- 6866.
- [26] G. Vall-Ilosera, B. Gao, A. Kivimäki, M. Coreno, J. Álvarez Ruiz, M. de Simone, H. Agren, E. Rachlew, *J. Chem. Phys.*, **2008**, 128, 139901.